



DaNUbs

EVK1-CT-2000-00051

DELIVERABLE 2.1 – EVALUATED MODEL ON ESTIMATING NUTRIENT FLOWS DUE TO EROSION/RUNOFF IN THE CASE STUDY AREAS SELECTED

Peter Strauss, Gabriele Wolkerstorfer

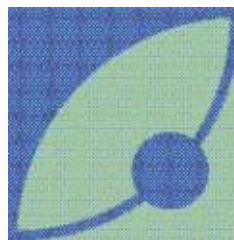
**Institute for Land and Water Management Research, Federal Agency for Water
Management, A-3252 Petzenkirchen**

peter.strauss@baw.at

Kalman Buzas, Adam Kovács, Adrienne Clement

**Department of Sanitary and Environmental Engineering Technical Budapest
University of Technology and Economics**

buzas@vcst.bme.hu



1 INTRODUCTION.....	4
2 THE YBBS AND WULKA RIVER CASE STUDY	5
2.1 MODEL DESCRIPTION	5
MUSLE (Williams, 1982)	5
Modified Morgan-Morgan-Finney model (Morgan, 2001).....	7
2.2 DATA COLLECTION	11
2.2.1 Soils	11
Ybbs	11
Wulka	17
2.2.2 Climatic information	18
Ybbs	18
Wulka	18
2.2.3 Landuse	21
2.2.4 Slope.....	23
Ybbs	23
Wulka	23
2.3 BASIC VALIDATION AND CALIBRATION OF MUSLE AND MMF	27
2.3.1 Model validation	27
2.3.2 Calibration of erosion models at subbasin level	30
Ybbs	30
Wulka	32
2.4 SIMULATED SEDIMENT LOADS	33
2.4.1 5.1. Ybbs	33
MUSLE	33
MMF	34
Model Comparison and comparison of simulated and measured sediment loads	35
2.4.2 5.2. Wulka	38
MUSLE	38
MMF	39
Comparison simulated – measured sediment loads	40
2.5 SIMULATED PHOSPHORUS LOADS.....	41
MUSLE	42
MMF	46
3 THE ZALA RIVER CASE STUDY	52
3.1 DEVELOPMENT OF A SWAT SOIL DATABASE FOR THE UPPER WATERSHED OF RIVER ZALA (ABOVE ZALAAPÁTI) BY INCORPORATING DIFFERENT DATA SOURCES INTO GIS.....	53
3.1.1 New soil polygons derived from the dataset.....	55
3.1.2 Calculation of pedotransfer functions in sequence of the variables of SWATmodel.....	58
3.1.3 SWAT model application for Zala River catchment	67
Watershed characteristics	67

SWAT application	71
3.1.4 <i>Results, discussion and conclusions</i>	75
4 SUMMARY	80
4.1 EFFORTS TO DERIVE BASIC INFORMATION ON INPUT DATA FOR SOIL EROSION MODELLING FOR THE MESOSCALE	80
4.2 WORK TO SIMULATE SOIL EROSION AND PHOSPHORUS LOSSES WITHIN THE CASE STUDY CATCHMENTS; .	80
5 REFERENCES.....	83
6 APPENDIX.....	86

1 INTRODUCTION

Aim of this deliverable is to implement a comparative assessment of runoff, erosion and associated nutrient transport within the selected case study areas. Therefore two different modelling approaches have been used. Model calculations estimate sediment and nutrient flows due to soil erosion and surface runoff reaching the river. The case study catchments where work has been undertaken for this work-package were the Ybbs the Wulka and the Zala catchment. Beforehand an application of erosion models various steps of data collection and gathering had to be performed. This concerned mainly data to describe spatial properties of soil for all case study areas. However, methodological approaches at the different catchments are different due to different types of data availability. Concerning the problem of erosion estimation, two erosion models were compared, the so called MUSLE and MMF models (for a description see later chapters). At some parts of the report, reference will be made to the model USLE, which is in terms of structure and model parameters very similar to the MUSLE. This was done within various subcatchments of the Ybbs and the Wulka river. For the Zala river catchment efforts concentrated on application of the MUSLE. Obtained results were compared to calculated loads. Concerning the problem of nutrient input via erosion and surface runoff, both tested erosion models were connected to algorithms to calculate phosphorus loads. In the case of MUSLE results were obtained by using the nutrient transport component of the SWAT model. In the case of MMF results were obtained by coupling of sediment loads to calculated enrichment ratios of phosphorus in river sediment.

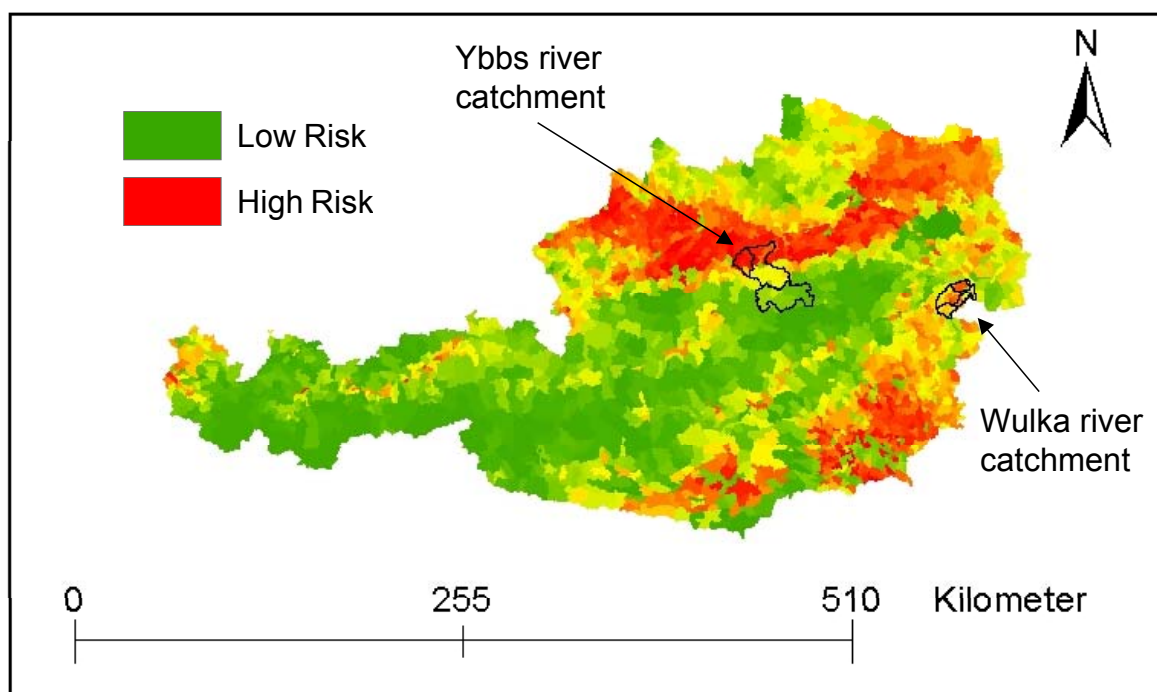
Acknowledgements

Digital elevation models, water quality data and water flow data were obtained from the Federal Governments of Lower Austria and Burgenland; Digital soil maps were partly obtained from Bundesamt und Forschungszentrum für Wald; Geological maps were partly obtained from Geologische Bundesanstalt; Climate data were obtained from Hydrographischer Dienst, BMLFUW. Data on plant available P were given by AGES. Soil data of BZI were obtained by Umweltbundesamt and the governments of the Federal provinces of Lower Austria and Burgenland.

2 THE YBBS AND WULKA RIVER CASE STUDY

Although the Ybbs river and the Wulka river catchments are quite different in terms of geomorphological and climatic background, they can both be considered as being sources of sediment production as can be demonstrated by Figure 1, which gives a rough estimate on areas in Austria endangered by soil erosion through water.

Figure 1: Location of the Austrian case study areas with respect to soil erosion risk by water (Strauss, in preparation)



2.1 Model Description

2.1.1 MUSLE (Williams, 1982)

The MUSLE is a modified version of the well known USLE (Wischmeier and Smith, 1978). The main difference compared to the USLE is the replacement of the so called rainfall factor with a direct estimate of surface runoff and peak runoff rate. In addition the temporal resolution of the calculations is daily, whereas the USLE gives long term annual means. The authors claim that the introduction of direct estimates for surface runoff allows the extension of the original USLE to calculate sediment deposition. The MUSLE was used as incorporated in SWAT (Neitsch et al., 2001), which is a GIS integrated software tool to calculate water and nutrient flows in large catchments.

Further details on SWAT may be found in Deliverable D 1.1. on water balance calculations in the case study areas and on the SWAT homepage at <http://www3.baylor.edu/cagsr/swat/>.

2.1.2 Input parameters for the MUSLE model

The basic equation to calculate sediment loss is

$$SED = 11.8 * (Q_{surf} * q_{peak} * Area_{hru})^{0.56} * K_{USLE} * C_{USLE} * P_{USLE} * LS_{USLE} * CFRG \quad 1)$$

where:

SED = sediment loss (metric t)

Q_{surf} = surface runoff (mm/ha)

q_{peak} = maximum surface runoff ($m^3 s^{-1}$)

$Area_{hru}$ = Area of a hydrological response unit (km^2)

K_{USLE} = K-Factor of the USLE ($t h ha^{-1} N^{-1}$)

C_{USLE} = C-Factor of the USLE (dimensionless)

P_{USLE} = P-Factor of the USLE (dimensionless)

LS_{USLE} = LS-Factor of the USLE (dimensionless)

CFRG = coarse fragment factor of the USLE (%)

A set of additional variables is necessary to calculate these factors.

Table 1 gives an overview about these additional input parameters and their units for application of the model.

Table 1: Additional input parameters for application of the MUSLE

Factor	Additional Input Parameter	Unit
Q _{surf}	Daily rainfall	mm
	Hydrologic soil group	-
	Soil water content at saturation	mm
	Soil water content at field capacity	mm
	Usable soil water content of soil profile	mm
	Land use	-
	q _{peak}	Time of concentration
Extreme amount of 0.5 h rainfall for a given month		mm
Average amount of 0.5 h rainfall for a given month		mm
K _{USLE}	Organic carbon content of upper soil layer	%
	Soil permeability	-
	Percentage of soil particle size < 50 µm	%
	Percentage of soil particle size < 125 µm	%
	Percentage of soil particle size < 2 µm	%
C _{USLE}	Soil structure code	-
	Soil cover for different periods throughout the year	-
P _{USLE}	Relative contribution of rainfall energy for different periods of the year	-
	Table values	-
L _{USLE}	Slope	(m/m)
	Hillslope length	m
CFRG	Rock content of upper soil layer	%

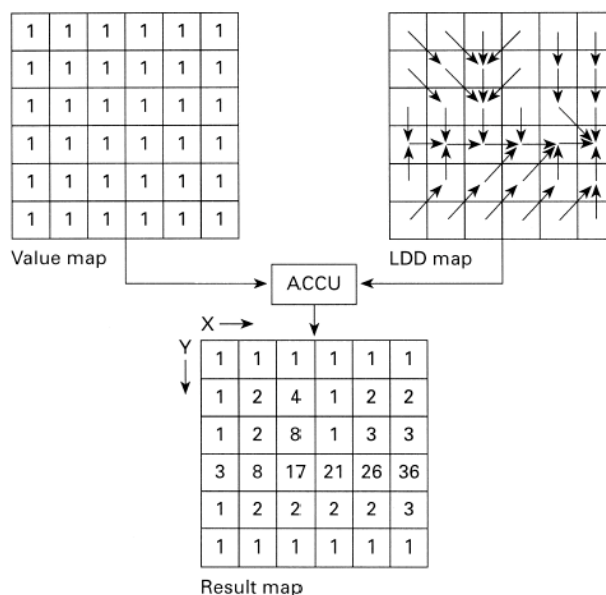
2.1.3 Modified Morgan-Morgan-Finney model (Morgan, 2001)

This model is a revised development of the original Morgan-Morgan Finney model (Morgan et al., 1984). For ease of reading it will be referred as MMF model in the text. It was developed to predict long term erosion rates at field scale and small watershed level. It tries to put the basic relationships of erosion and runoff into process which are described by various mathematical functions. Basic ideas of the modelling approach are taken from the concepts of Meyer and Wischmeier (1969)

and Kirkby (1976). The model separates the erosion process into two processes, the water phase and the sediment phase. The eroded sediment is compared to the transport capacity of the runoff and the smaller value is taken as mean soil loss/year. A flow diagram of the processes involved is given in Figure 3. One modification of the chosen model for this analysis was done by using monthly calculations of the necessary input parameters. Monthly soil loss rates were then summed up to get annual soil loss. As monthly rainfall amounts were available we took these instead of the methodology proposed in the original model which uses mean annual rainfall and a mean number of days with rainfall. This does not necessarily result in a better model performance but enables to account for a better model response to the highly variable environmental conditions throughout the year and therefore makes simulations more realistic. Similar assumptions were underlying the introduction of the explicit runoff term in the MUSLE wherein surface runoff is calculated with daily rainfall values.

Due to the large size of the case study areas a second main modification of the MMF model was to incorporate it into a GIS. The chosen GIS was the grid based PCRaster (Van Deursen, 1995). According to the grid structure of PC Raster, all necessary input variables had to be supplied for each grid cell. The chosen grid size of 25 m for the Ybbs river and 50 m for the Wulka river corresponds to the available DEM data for these areas. The relatively dense format of DEM data justified to calculate surface runoff and erosion in a spatially distributed way. This means that calculations for surface runoff and erosion were not done independently for each grid cell, but surface runoff and erosion were routed along the different grids until a stream was reached. Various algorithms exist to route surface runoff within watersheds. The one implemented here is called steepest descent (Jenson and Domingue, 1988). The basic assumption of this algorithm is that one grid cell drains completely into one other cell. Therefore one grid cell may receive input from more than one upstream cells but may deliver only to one downstream cell. The decision about which cell delivers into another is based on slope and aspect. Along its flowline, runoff and erosion are accumulated until the end in a stream. No processes take place in stream and all sediment that enters the stream is delivered to the outlet. Figure 2 gives an overview of the routing scheme which has been implemented. Further details about PCRaster and the implementation of the MMF model may be found at <http://pcraster.geog.uu.nl/> and Wolkerstofer (2002).

Figure 2: Schematic representation of routing in the MMF model as incorporated into PCRaster



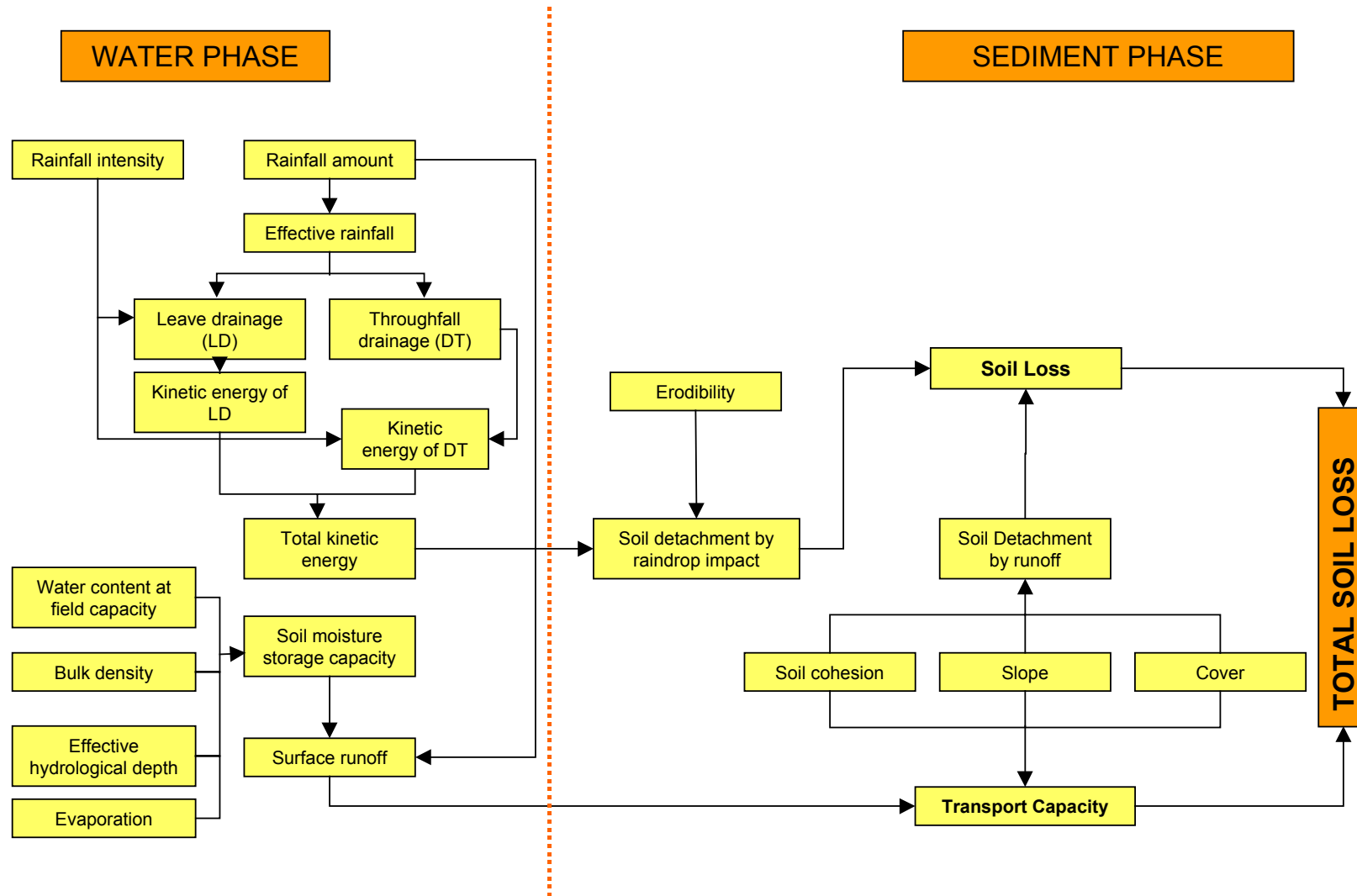
2.1.4 Input parameters for the MMF model

Table 2 gives the necessary input parameters and their units for application of the model.

Table 2: Input parameters and their units for the MMF model

Factor	Parameter	Unit
Rainfall	Annual or mean rainfall	mm
	Number of rain days/year	-
Soil	Soil moisture content at field capacity or 1/3 bar tension	%w/%w
	Bulk density of the top soil layer	Mg/m ³
	Effective hydrological depth of soil	m
	Soil detachability index	g/J
Landform	Cohesion of the surface soil	kPa
	Slope steepness	degree
Land cover	Proportion of rainfall intercepted by vegetation	%/100
	Ratio of actual to potential evapotranspiration	%
	Ground cover	%
C _{USLE}	Soil cover for different periods throughout the year	-
	Relative contribution of rainfall energy for different periods of the year	-
	Plant height	m

Figure 3: Flow chart of the MMF model



2.2 Data collection

2.2.1 Soils

Ybbs

At present several data bases to obtain soil information exist in Austria (Schwarz et al., 2001). However no digital version of any spatially distributed data base except the European soil map (ESB, 1998) existed for the catchment of the river Ybbs. Unfortunately, the scale of this map is rather large and therefore it is not suitable for an application and modelling of soil erosion within watersheds of the selected size. Additional efforts were put into the development of spatially distributed soil data with a higher spatial resolution compared to the European soil map. The methodology applied is given in Figure 5. It consisted in a combination of data which were available spatially distributed (geological maps, which partially have been purchased, partially had to be put into digital format by ourselves) with data that allowed to quantify particular soil properties. The latter information was taken from table values of the Austrian soil mapping system. Details about types and extent of information which can get extracted from these data is given by Schneider et al. (2001). The basic soil map which has been obtained with this methodology is shown in Figure 6. Geological maps as well as soil maps are dissected into units of various size, herein geological information was connected to soil characteristics and slope. An additional challenge was to unify these sections. This was complicated by the fact that the various experts who had collected the data used different technical terms for similar data. Beside obtaining basic soil information for various water balance calculations, main purpose of our work was to derive spatially distributed information about soil erodibility. Unfortunately only basic soil properties are described within the Austrian soil mapping system data base. The MMF model and the MUSLE require different input parameters for the quantitative description of soil erodibility. For obtaining soil erodibility values to be used in the MUSLE it was necessary to develop transfer functions. Calculation of soil erodibility in the MUSLE is based on the equation (Wischmeier and Mannering, 1969).

$$K = 2.77 \cdot 10^{-6} \cdot M^{1.14} \cdot (12 - OS) + 0.0043 \cdot (A - 2) + 0.033 \cdot (4 - D) \quad 2)$$

where:

K = Soil erodibility factor ($t \text{ h ha}^{-1} N^{-1}$)

M = (%silt+%finest sand)*(100-%clay)

OS = % organic matter

A = size of aggregates

D = permeability class

We used soil information of a set of rainfall simulation experiments to compare the necessary soil properties with soil properties which are available at the level of the Austrian soil mapping system. These experiments had already been conducted in previous years. A regression analysis revealed a strong dependency between K-factors obtained via original equation and soil silt contents (Figure 4). Similar findings for the correlation between soil silt content and the K-factor has also been obtained by other work in Europe (Meyer, 1997). Therefore as a surrogate for the K-Factor calculation using detailed soil information the silt content after obtaining a relationship from rainfall simulations can be used.

$$\text{K-Factor} = 0.0083 (\pm 0.044) + \text{silt \%} \times 0.0086 (\pm 0.001), r = 0.91, n = 30 \quad 3)$$

However, it should be noted that this equation is only valid under the assumption, that the K-Factor calculation in the MUSLE is correct. This is not the case for certain conditions as will be shown in the chapter on validation. However, available data do not allow to modify this. Users of the USLE, MUSLE or its derivatives should be aware of this.

The obtained K-factors were further modified by inclusion of the rock contents of the upper soil horizon. The semiquantitative information from the Austrian soil mapping system on volumetric rock content of the various layers of a profile was transformed into quantitative information according to Table 3.

Table 3: Transformation of semiquantitative data given in the Austrian soil mapping system on rock content into quantitative data

Mapping Description	Mapping value %	Rock _V (Vol %)	Rock _M (Mass%)
No rock content	-	0	0
Low rock content	0-10	5	8
Moderate rock content	10-20	15	23
High rock content	20-40	30	45
Very high rock content	40-70	55	83
Predominate rock content	>70	85	100

The volumetric rock content was transformed into mass percentages based on the assumption of a mean density relationship of $\rho_{\text{fine earth}}/\rho_{\text{stone}} = 0.66$ (Torri et al., 1994, modified).

Finally, reduction of soil erodibility due to increasing rock content was included in the K-factor calculation according to Auerswald (1997).

$$\text{K-Factor}_{\text{mod}} = \text{K-Factor} \cdot (1 - 0.018 \cdot \text{Rock}_M + 0.00009 \cdot \text{Rock}_M^2); \text{Rock}_M \leq 83 \quad 4)$$

Figure 4: Relationship between calculated K-Factor according to Wischmeier and Smith (1987) and soil silt contents

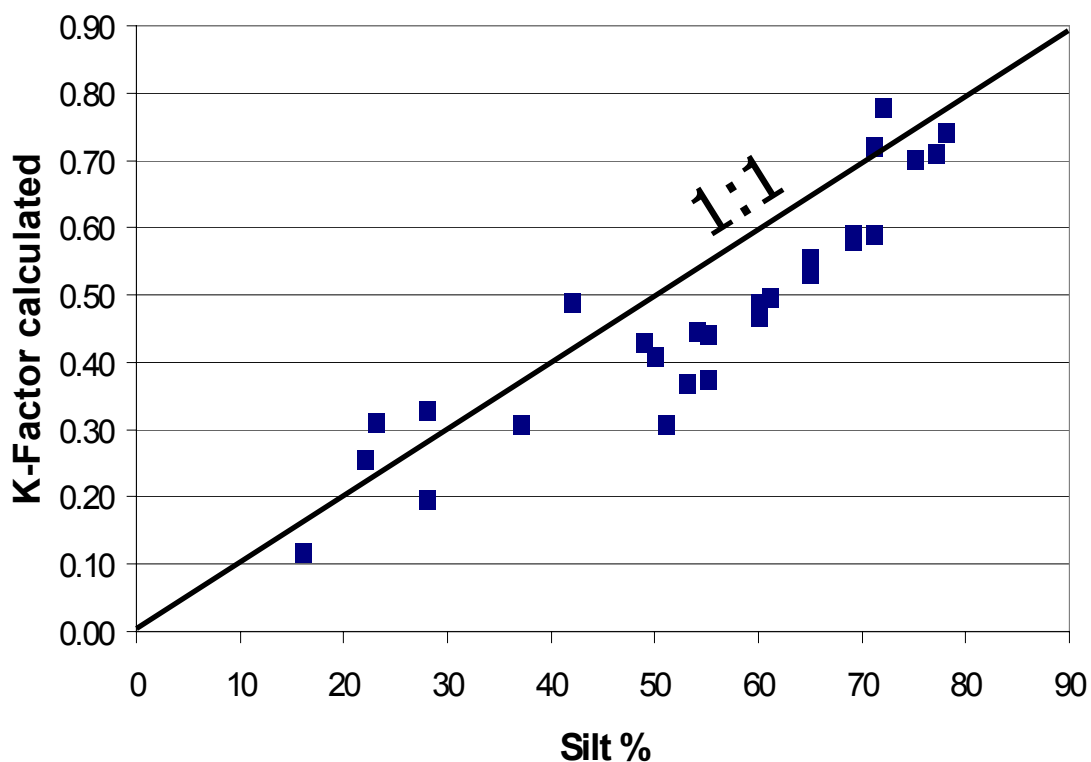
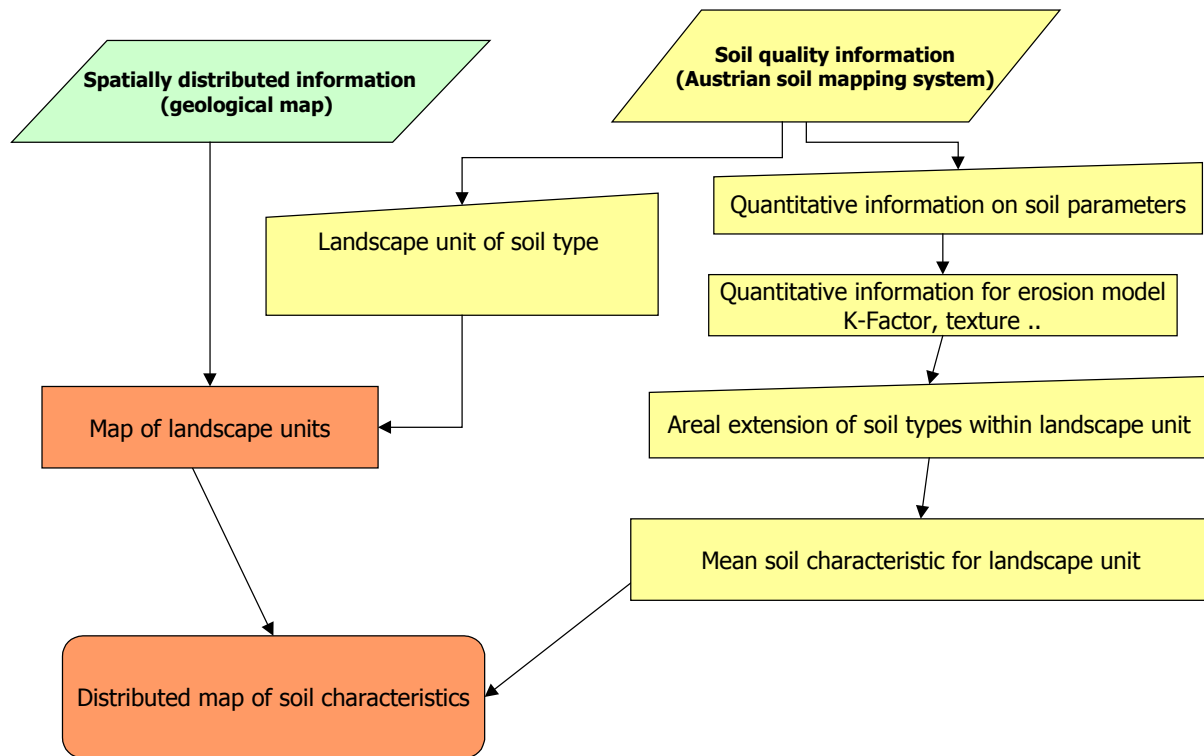


Figure 5: Methodology used to develop spatially distributed information on necessary soil data to quantify the influence of soil properties on soil erosion



Combination of the methodology given in Figure 5 with the K-Factor calculation resulted in a K-Factor map for the Ybbs river watershed which could be used as input for the MUSLE. Information on soil parameters in the Austrian soil mapping system is only available for agriculturally used land (codes 7, 9, 10, 14 in Table 4.). Therefore in a final step all other types of landuse were given a value of 0.05 K units to obtain Figure 7. Similar calculation based on little soil information and the compared results of erosion plot simulations can easily be gained on sites were soil information is rare or to evaluate the results of the K-Factor.

Figure 6: Basic soil map for the Ybbs river watershed (note that the names of the different soil units are compatible with international nomenclature but are composed of 3 parts: first part: Au - floodplain, Hochterrasse - high terrace, Molasse – molasse, Niederterrasse – low terrace, Flysch – Flysch, Kalk – limestone, Moor – Fen, Moraene, moraine; second part: KB Amstetten, KB Gaming, KB St.Peter refers to the name of the cartographic unit which has been used; third part: <math><15^\circ</math>, $>15^\circ$, $15-25^\circ$ refers to different slopes, that have been used for discretisation of soil units

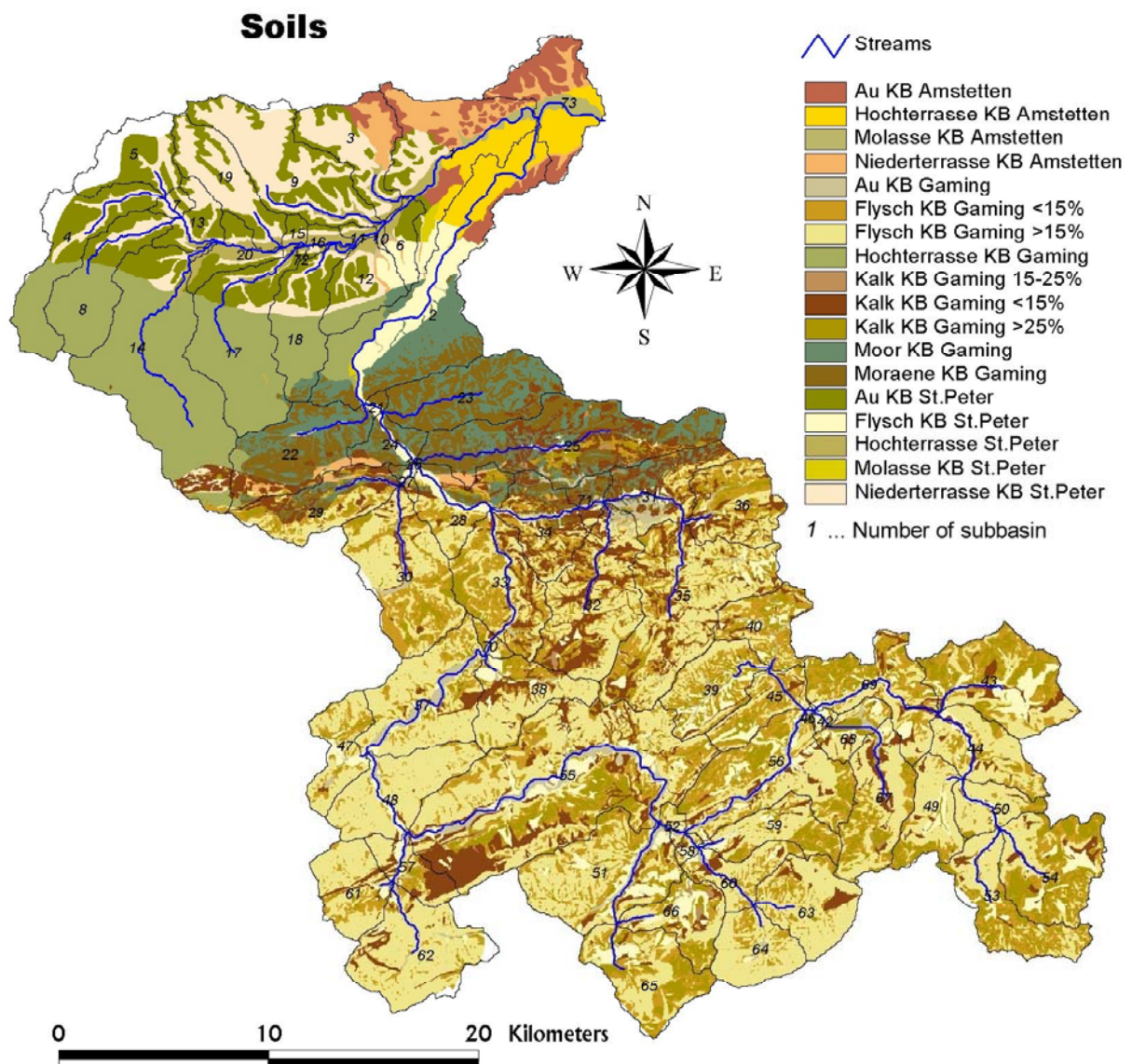
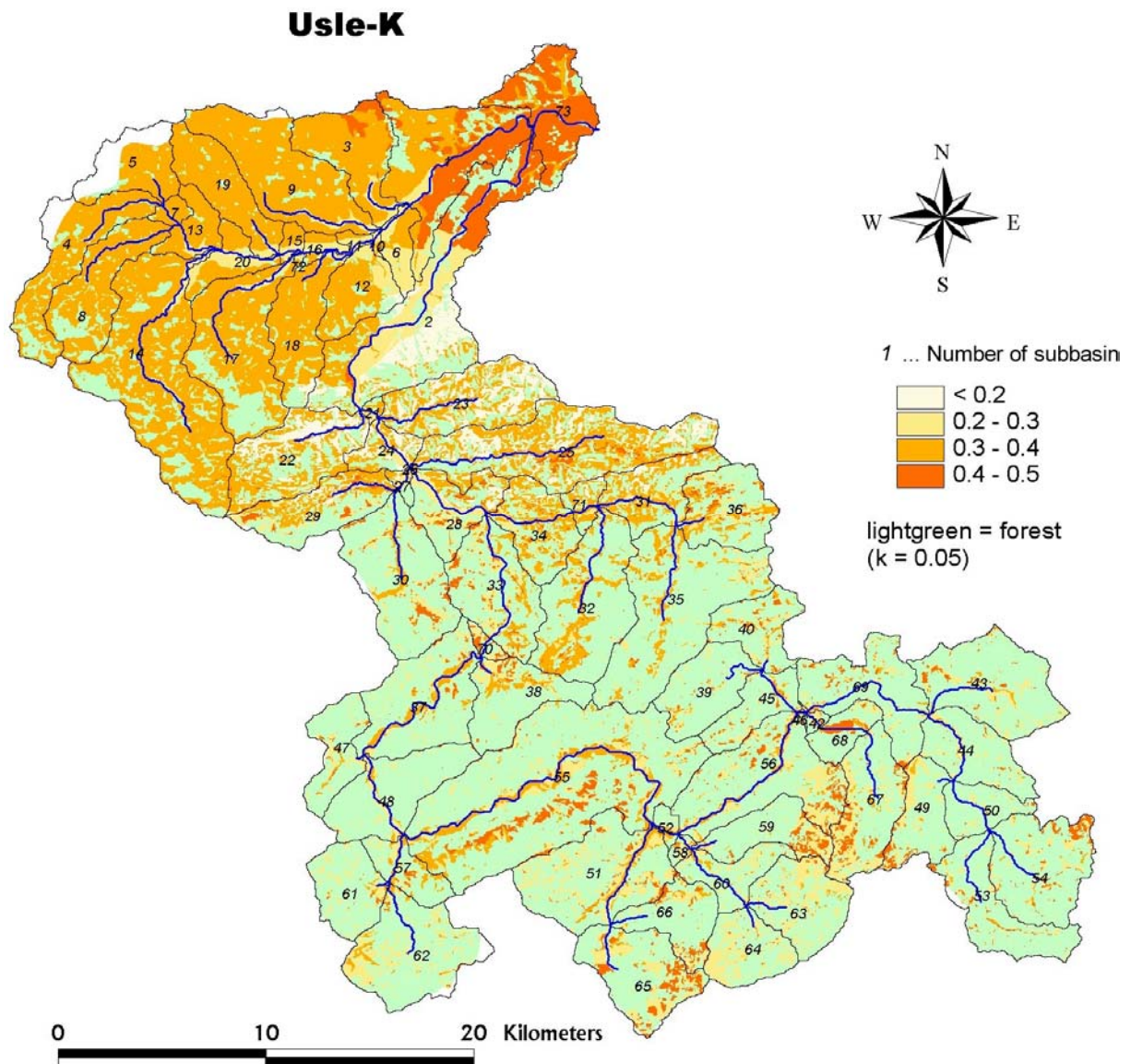


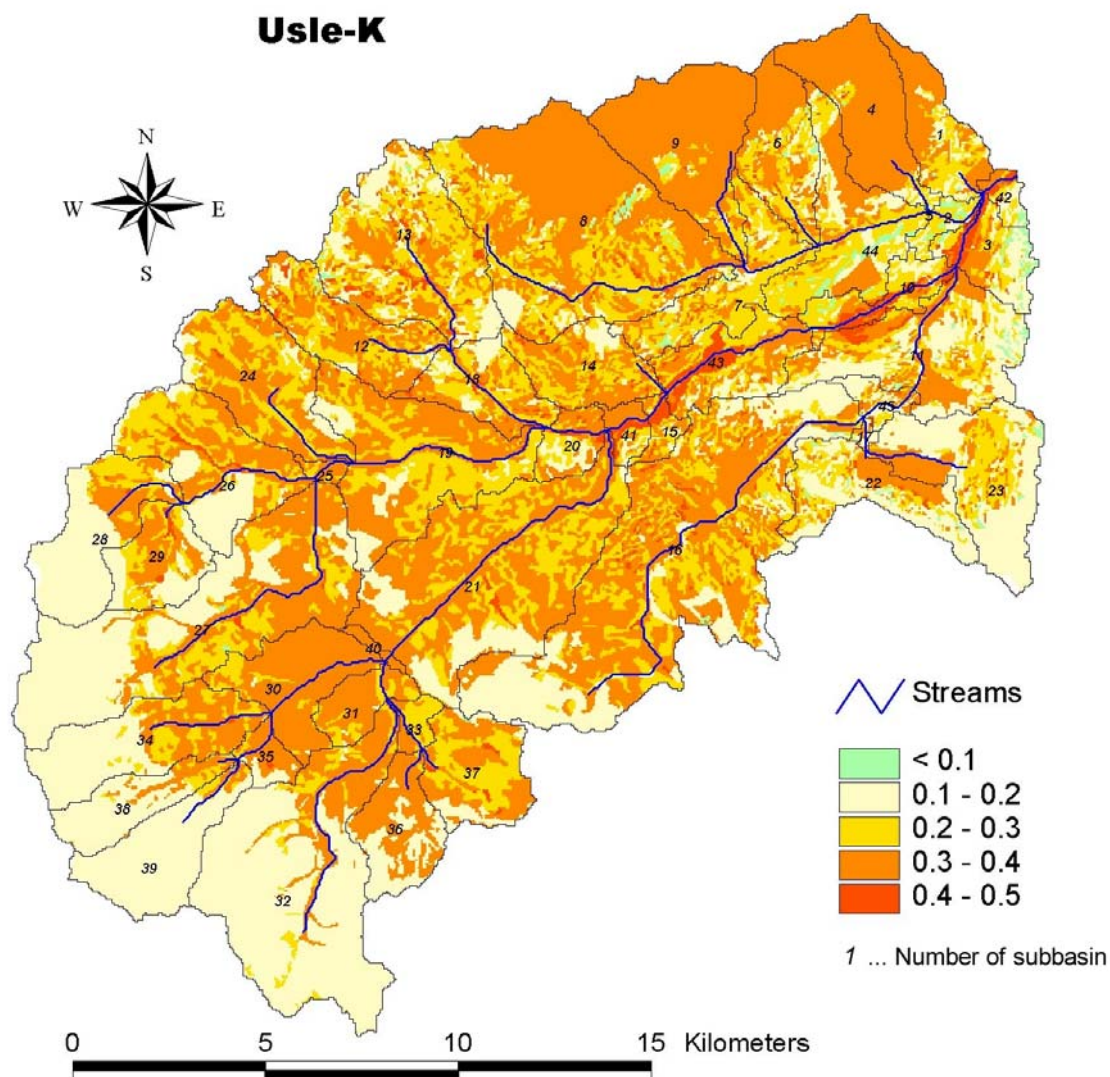
Figure 7: Distribution of the K-Factor_{mod} values within the Ybbs river watershed

In the case of the MMF model it was possible to use soil texture values directly or to derive soil parameters from a combination of land use and soil type. The tables of the appendix give the chosen input values for the different parameters of the MMF model.

Wulka

To obtain the necessary soil input parameters for the Wulka river catchment we used a digitally available data set of the Austrian soil mapping system directly (BFL, 1999; LVA, 1971). Therefore, no assumptions about the spatial distribution of the described soil units had to be done by using geological maps, but K-Factor values could be derived directly from these data but of course it was necessary to apply equations 3) and 4) to transform textural information into K-Factor values. Evaluation of soils under forest was done using data from the description of the forest soil mapping system (Mutsch, personal communication). Figure 8 gives the distribution of K-Factor values for the Wulka river catchment.

Figure 8: Distribution of $K\text{-Factor}_{\text{mod}}$ for the Wulka river catchment



2.2.2 Climatic information

Ybbs

Figure 9 gives mean annual precipitation amounts for selected subbasins of the Ybbs river catchment. The location of the climatic stations used for the calculations in the Ybbs river catchment can be obtained from the report on Deliverable 1.1. (Water balance calculations). The necessary input data for the MMF model were also derived from the same data. Data on actual and potential evapotranspiration were taken from the SWAT calculations. A modification to the original model was, that we did not use annual but monthly climatic information. In addition the model MMF uses mean rainfall intensity of atypical rain. Therefore more detailed information on a daily basis was needed. The rain intensity could be obtained by an evaluation of longer time series of rainfall at other monitoring stations, wherein the station Steyr was assigned to the subbasin Ybbs and the station Baden to the catchment area of the Wulka (Strauss et al, 1995).

Wulka

Figure 10 gives mean annual precipitation amounts for selected subbasins of the Wulka river catchment. The location of the climatic stations used for the calculations in the Wulka river catchment can be obtained from the report on Deliverable 1.1. (Water balance calculations).

Figure 9: Mean annual precipitation amounts for various subcatchments of the Ybbs river (Ø 91-97)

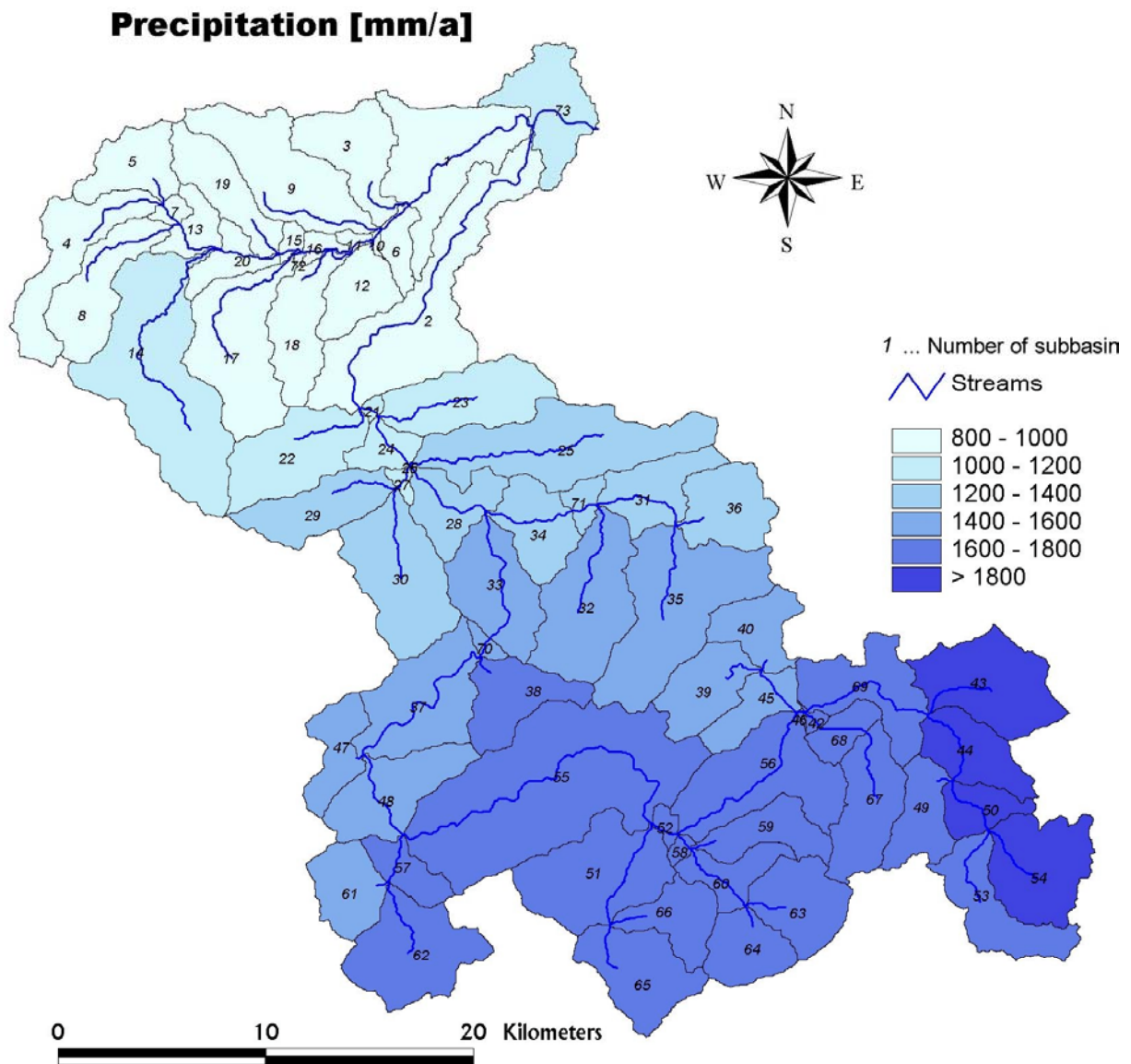
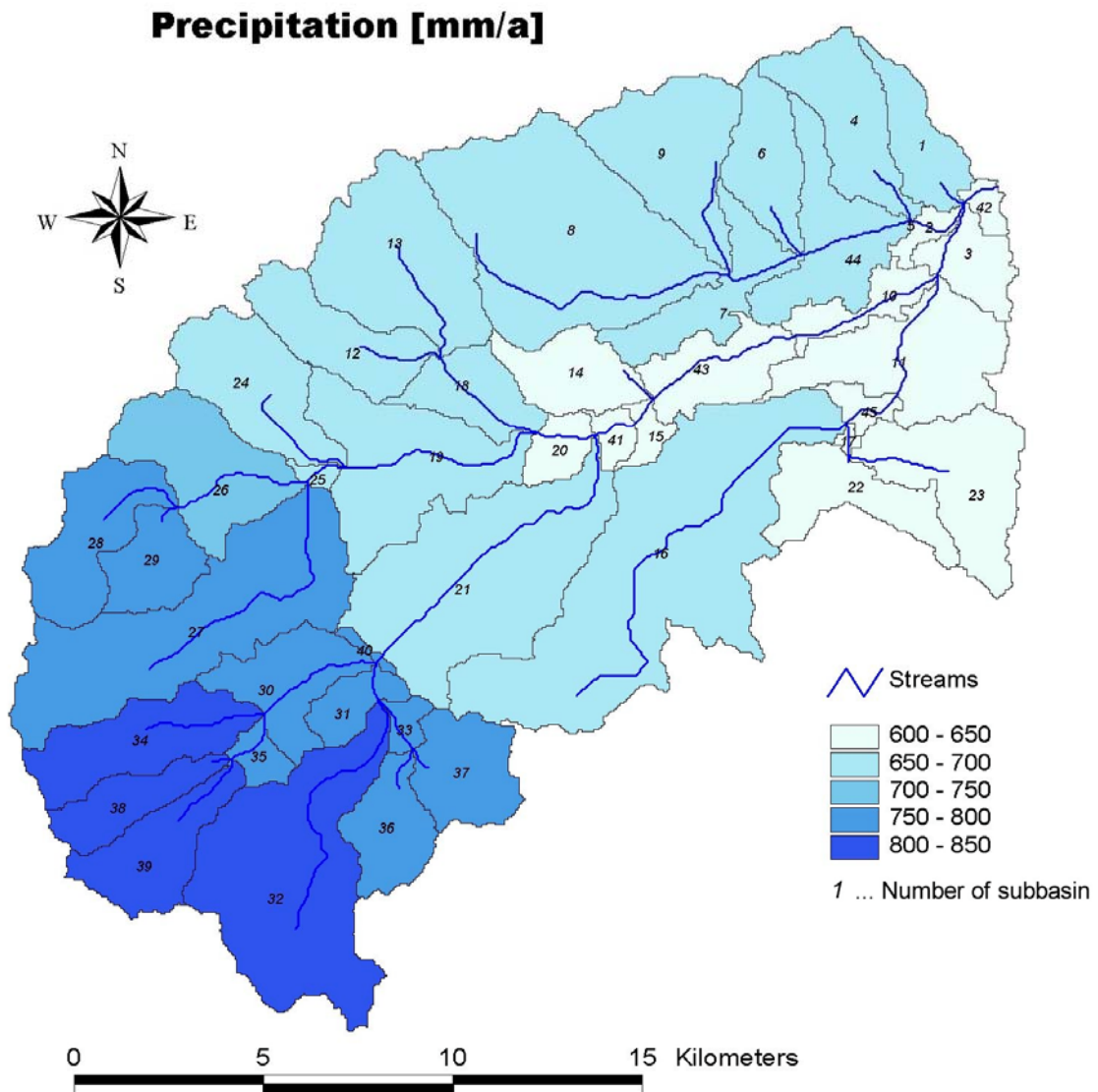


Figure 10: Mean annual precipitation amounts for various subcatchments of the Wulka river (Ø 92-97)



2.2.3 Landuse

Landuse characteristics were derived from a multi temporal evaluation (May 1999 and August 1999) of satellite data (LANDSAT-7) with a spatial resolution of 30 x 30 m. Aim of this evaluation was to obtain spatially distributed information about land-use characteristics which are important for the hydrologic behaviour and the susceptibility to erosion. Table 4 gives the classification scheme which was used. Technical details about the employed procedure can be obtained from the technical report on “Multisaisonale Landbedeckungsklassifizierung aus Satellitenbilddaten für die Einzugsgebiete Ybbs und Wulka“ given by the „Institut für Vermessung, Fernerkundung und Landinformation“. According to this classification scheme, the necessary input values for the MUSLE and MMF were derived. In the case of MUSLE, the C-Factors are calculated according to the equation

$$C_{USLE,mn} = 1.463 \cdot \ln(C_{USLE,AA}) + 0.1034 \quad 5)$$

Where

$C_{USLE,mn}$ = minimum value for C

$C_{USLE,AA}$ = average annual value for C

Only minimum values for C-factors are given in the parameter tables of SWAT. It is not possible to calculate mean annual values for the C-factor because the given equation results in wrong values. Because plant cover varies during the growth cycle of the plant, SWAT updates C-Factors daily using the minimum value for C.

For the case of the MMF model, selection of the various input parameters was partly based on expert knowledge partly table values of other erosion models have been used (Schmidt et al., 1996). The chosen input parameters are given in Table 22 and Table 23 of the appendix.

Table 4: Classification scheme for the multi temporal evaluation of Landsat-7 images for the catchments of the river Ybbs and Wulka.

Code	Name	Description
1	<i>Rock</i>	Areas with rocks; partially (most of all in mountainous areas) also roads and ways are classified as rock; interpretation errors with gravel are possible;
2	<i>Gravel</i>	Gravel areas; sandy uncovered soils; interpretation errors with rock are possible.;
3	<i>Area without vegetation</i>	Soils without vegetation at both times; may also be construction sites (industrial sites), interpretation errors with gravel or rock are possible;
4	<i>Water</i>	Areas covered with water, open water areas like lakes, but not mixed areas of water with attached vegetation, for instance narrow water bodies in riparian zones;
5	<i>Reed</i>	Areas covered with reed, wet areas, wet areas with a high percentage of biomass;
6	<i>Coniferous forest</i>	areas covered with coniferous trees – cover > 40% (percentage of deciduous forest < 20%);
7	<i>Mixed forest</i>	Mixed forest– cover > 40%;
8	<i>Deciduous forest</i>	Deciduous forest – cover > 40%; this class also includes mixtures of low woods;
9	<i>Crop-wheat</i>	Crops like wheat, rye, barley and similar
10	<i>Crop- maize</i>	Crops like maize, sugarbeet and potatoes
11	<i>Permanent pasture</i>	Pasture with a high percentage of biomass at both times of image;
12	<i>Low biomass</i>	Pasture with little biomass at both times of image; this class also includes mountainous areas with little biomass; further this class includes a set of mixed pixels between for instance crop-maize and crop wheat or permanent pasture and roads, construction sites or similar;
13	<i>towns</i>	Towns, villages and similar
14	<i>Vineyard*</i>	Areas covered with wine, partially vineyards are also classified as areas without vegetation;
15	<i>Clouds, shadows</i>	Areas which could not be classified because of being covered at both image times with clouds or their shadows;

*) In the Wulka river catchment this class may also contain vineyards with additional vegetation below

2.2.4 Slope

Ybbs

Information on slopes consisted in a digital elevation model with a resolution of 25 m which was transformed into values of slope on a subbasin level for the MUSLE application within SWAT (Figure 12). For the application of the MMF model actual grid values with the resolution of 25 m were taken as input.

Wulka

Information on slopes consisted in a digital elevation model with a resolution of 50 m. An procedure identical to the Ybbs river catchment was applied (Figure 13). Anyway, it should be noted, that due to the coarser resolution of the input data, a scaling error has to be expected. To get an impression about mean errors we therefore calculated mean slopes of the Ybbs river catchment on a subbasin level using different grid sizes. Figure 11 reveals the relationship between mean slope of the subbasins within the Ybbs river catchment and the grid resolutions of 25m, 50m, 100m, 200m, and 400m. As expected, the slope tends to smooth out at coarser grid sizes. The extent of this effect is dependant on the degree of steepness. Based on the findings on decrease of slope with increasing grid size it is possible to develop equations which may be used to correct different grid sizes. However, as the difference between a 25m grid and a 50 m grid was only about 5-10% for the range of slopes in the Wulka river catchment, and the effects on calculated soil loss was low, we did not set up such kind of equations to correct these data. But this fact should be taken into account by all modelling procedures: the coarser the spatial resolution is the higher is the error underlying an logarithmic relation. A set of equations to correct mean slope of catchments when only coarse grid data are available is proposed in Deliverable D 2.2.

Figure 11: Effect of different grid size on mean slopes at the subbasin level of the Ybbs river watershed, bars indicate standard deviation. Effect of slope changes on soil loss calculated with the USLE, using a high erosion risk assumption (high) and a low erosion risk assumption (low).

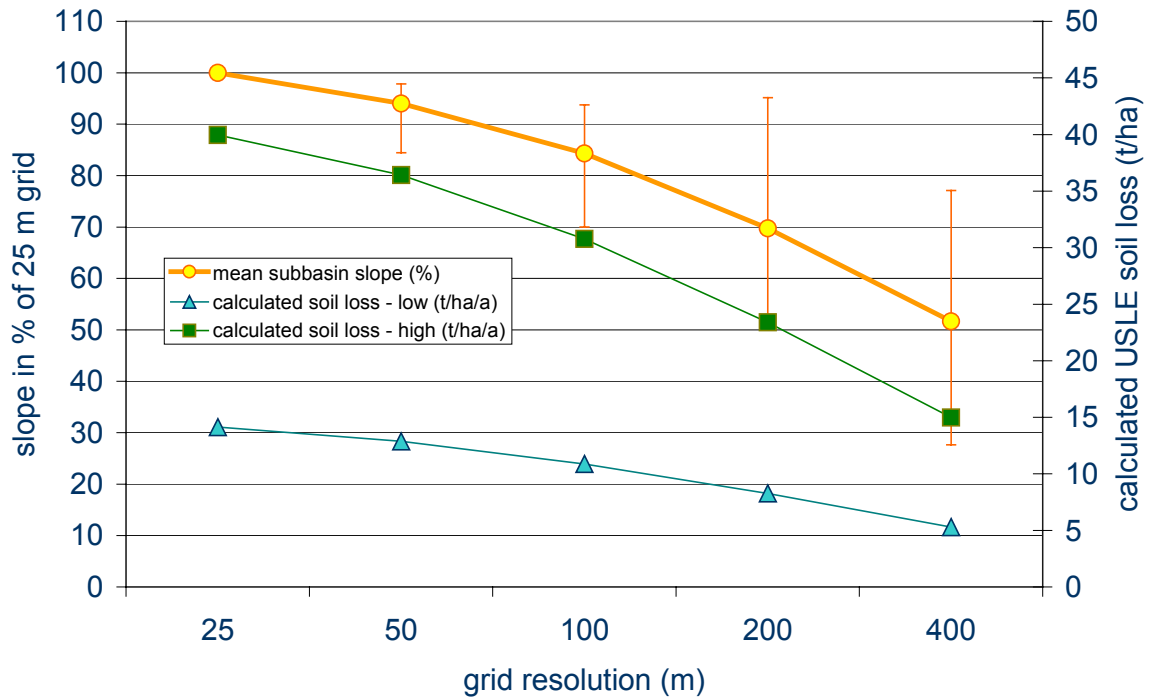


Figure 12 : Mean slope (°) within the Ybbs river catchment at the level of subbasins

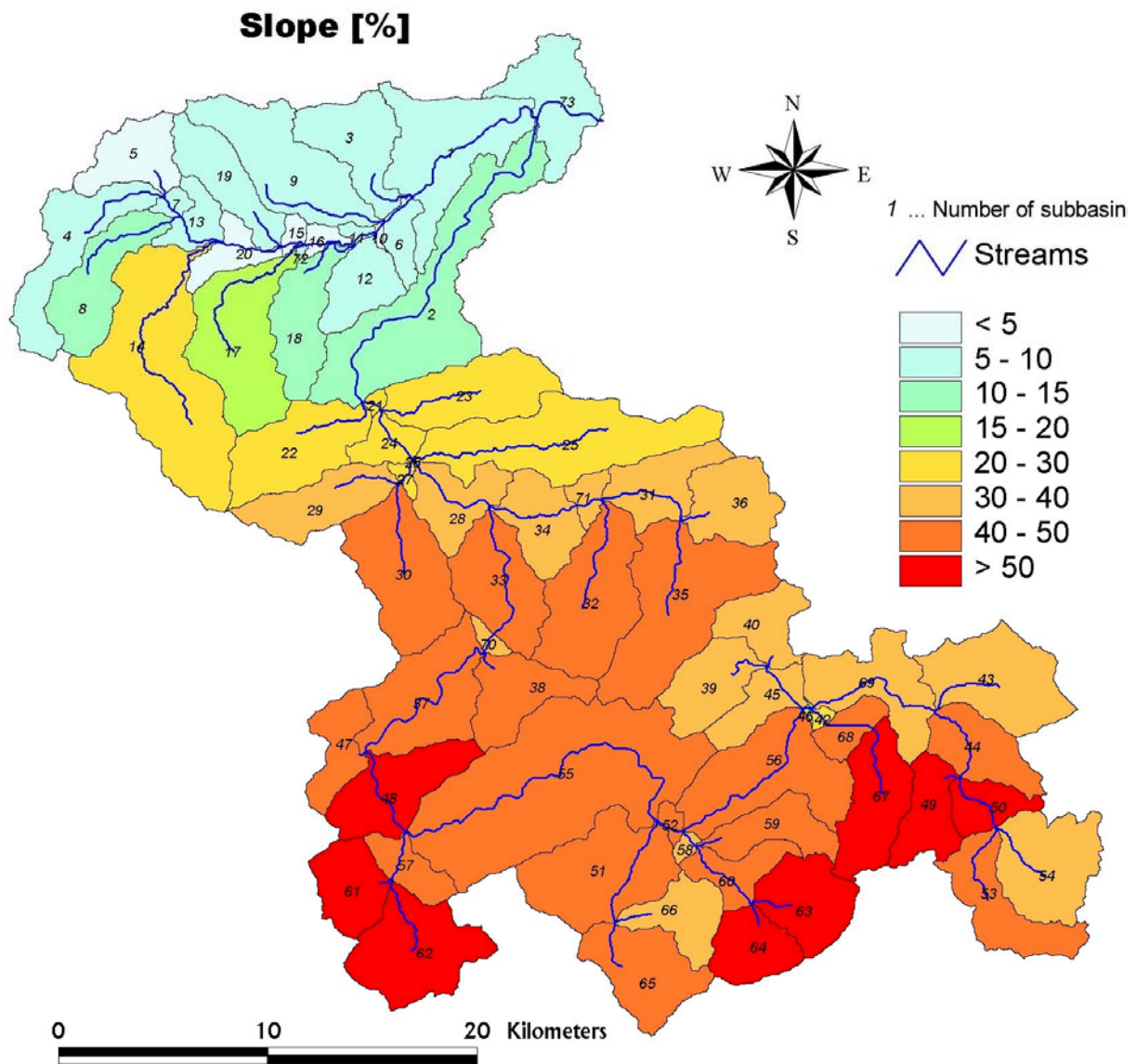
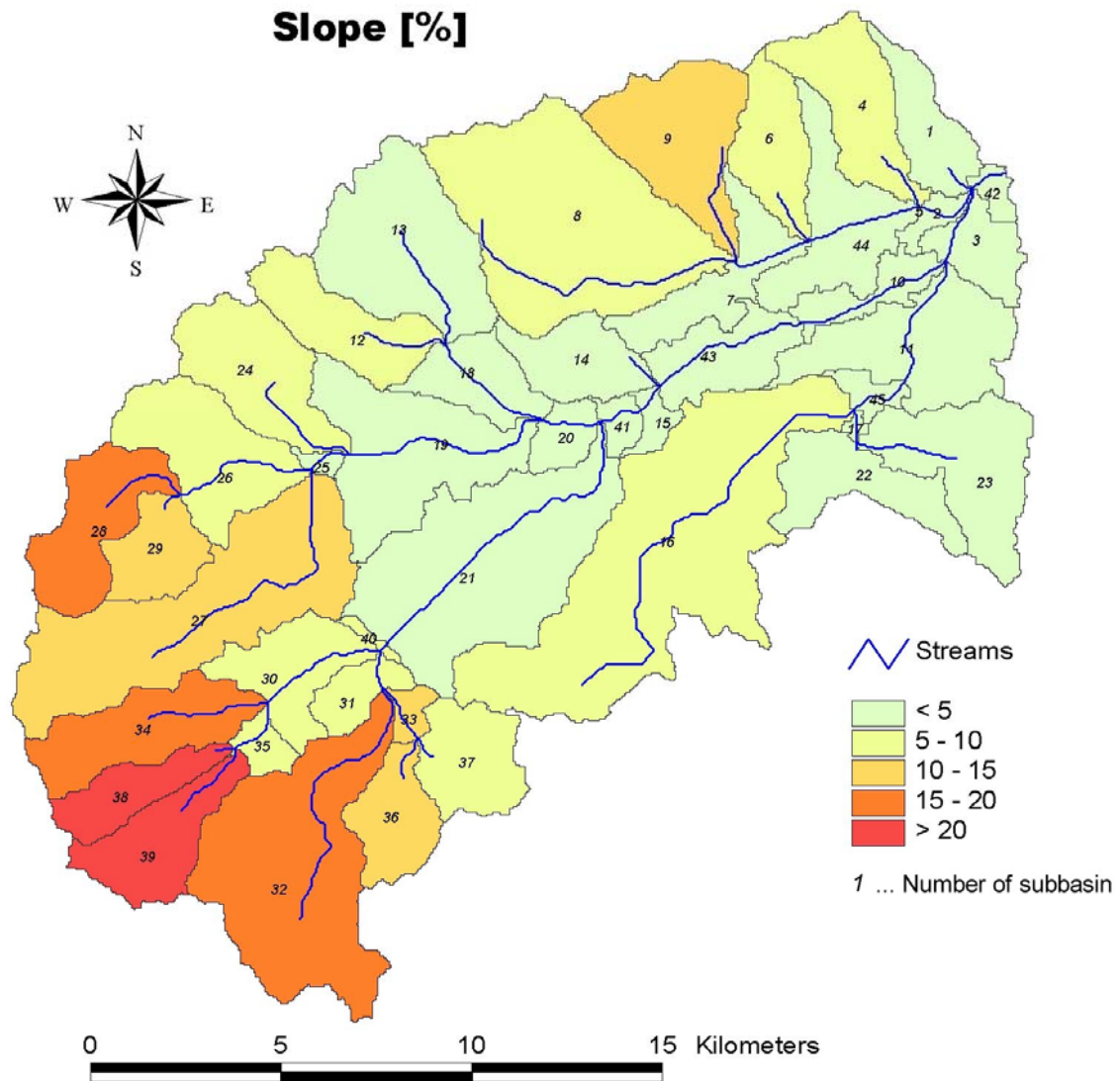


Figure 13: Mean slope (°) within the Wulka river catchment at the level of subbasins

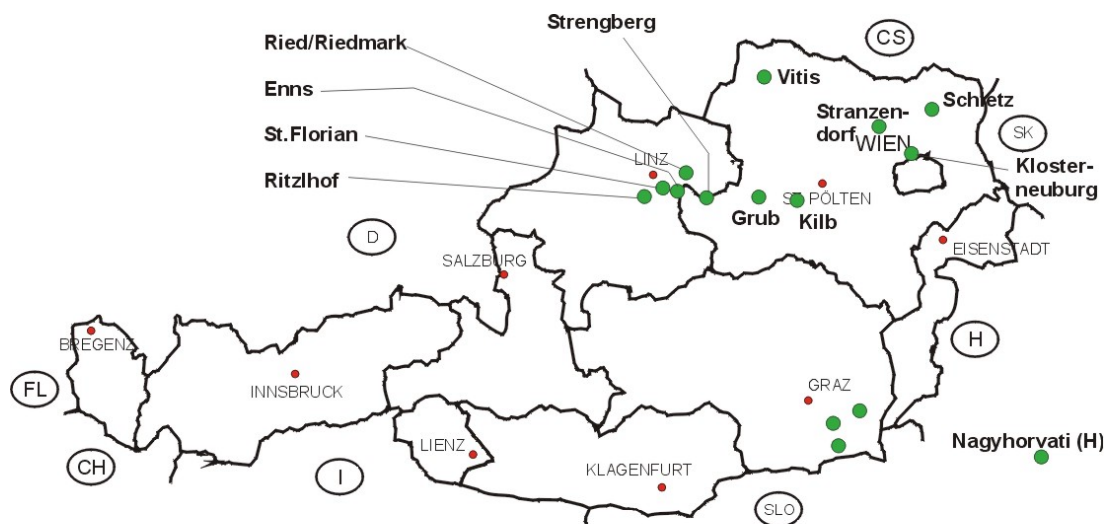


2.3 Basic validation and calibration of MUSLE and MMF

2.3.1 Model validation

The generic use of the models MMF and MUSLE in Austria and the application of parameters, process factors and basic assumptions used by the soil erosion model can be sampled best at research plots. To prove the validity of the assumptions within MUSLE and MMF we carried out an evaluation where measured data on rainfall simulation plots were compared to results obtained applying both models. Results on these rainfall simulation experiments had been obtained in previous years. The project gave the possibility to evaluate them for the first time together because relatively little information is available about the overall accuracy of the MUSLE in predicting soil loss especially on regional scale. This is due to the fact that it is complicated and cost-intensive measuring soil erosion for more than field size and only few possibilities exist to validate soil erosion in a spatially distributed way.. The sites where the experiments had been done are given in Figure 14.

Figure 14: Sites at which rainfall simulation experiments have been conducted



Plot sizes for the experiments varied between 10 m² and 12 m². A range of different soils occurring in those Austrian regions with the highest erosion risk was used. Only experiments which had been conducted at soil conditions corresponding to freshly prepared seedbed conditions were taken into consideration. For a first evaluation all other results were excluded from the analysis. Furthermore, mean values have been calculated whenever different treatments had been applied to one soil at the same

site (different rainfall intensities or similar). Evaluation was only performed on the soil erosion component of both models, which means that values for runoff were not estimated but supplied from rainfall simulation results. In a first attempt we focused on the K-factor which describes the influence of soil properties on soil loss.

Figure 15 gives the result for the comparison of measured erosion data with calculated erosion data using the MUSLE and USLE. From Figure 15 it can be concluded, that both approaches exhibit a directed error in the range of higher soil losses. Wischmeier and Smith (1976) calculate a mean deviation between measured and calculated soil loss of $0.31 \text{ kg m}^{-2} \text{ a}^{-1}$. Similar results have been obtained by Risse et al. (1993) using a similar data set to that of Wischmeier and Smith (1976). A comparison between measured K-factor values and USLE calculated K-factor values gives a correlation coefficient of 0.71 ($n = 26$) and a mean standard error for the prediction of K-factor values of 0.13. The implication of this result is that for any model application the K-factor cannot be estimated with a higher precision than K-factor ± 0.063 (68 % probability), and any grouping of these data needs to take that into account. But this applies only for the case where exact measurements of the necessary input data for K-Factor calculation are available. For any application beyond this, this precision has to be seen as a “best case” assumption. The relationship between measured soil loss and soil loss resulted in the linear regressions (no intercept included) of (6 and (7.

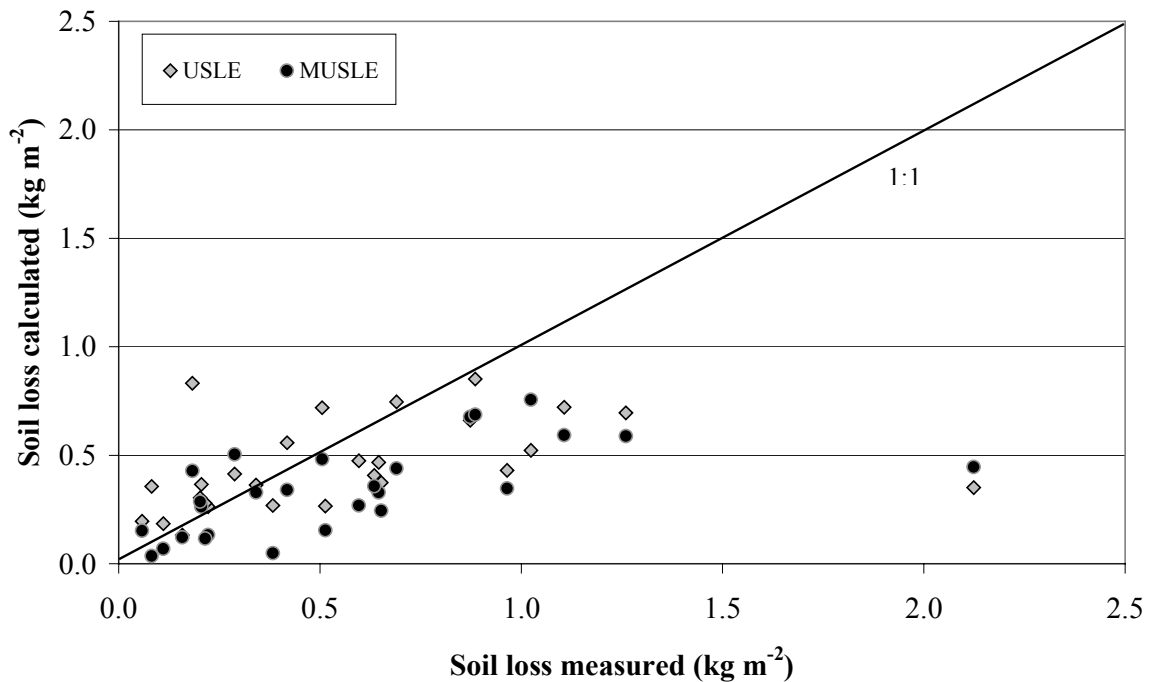
$$\text{Soil loss (USLE)} = 0.73 (\pm 0.07) * \text{measured soil loss} (n = 26, r = 0.61) \quad (6)$$

$$\text{Soil loss (MUSLE)} = 0.60 (\pm 0.05) * \text{measured soil loss} (n = 26, r = 0.75) \quad (7)$$

The slopes of (1) and (2) indicate a directed underestimate of both models. While Yoder et al. (2001) expect a more or less similar accuracy of the USLE for soil loss above $0.1 \text{ kg m}^{-2} \text{ ha}^{-1} \text{ a}^{-1}$, Figure 15 suggests a strong underestimation of soil loss, especially for the higher soil losses. Regression analysis with intercepts included reveals intercepts well above zero. This indicates a tendency to overestimate soil loss at low rates of soil erosion, a result that had also been obtained by Risse et al. (1993). Although the data set which was used for this analysis is certainly limited in terms of available replicates and temporal extension, it confirms results obtained elsewhere, indicating that, even with a high knowledge of input data, an application of

the USLE and its derivatives needs great care and is associated with considerable error.

Figure 15: Comparison of measured erosion data obtained via rainfall simulation experiments with calculated erosion data using the MUSLE and the USLE equations.

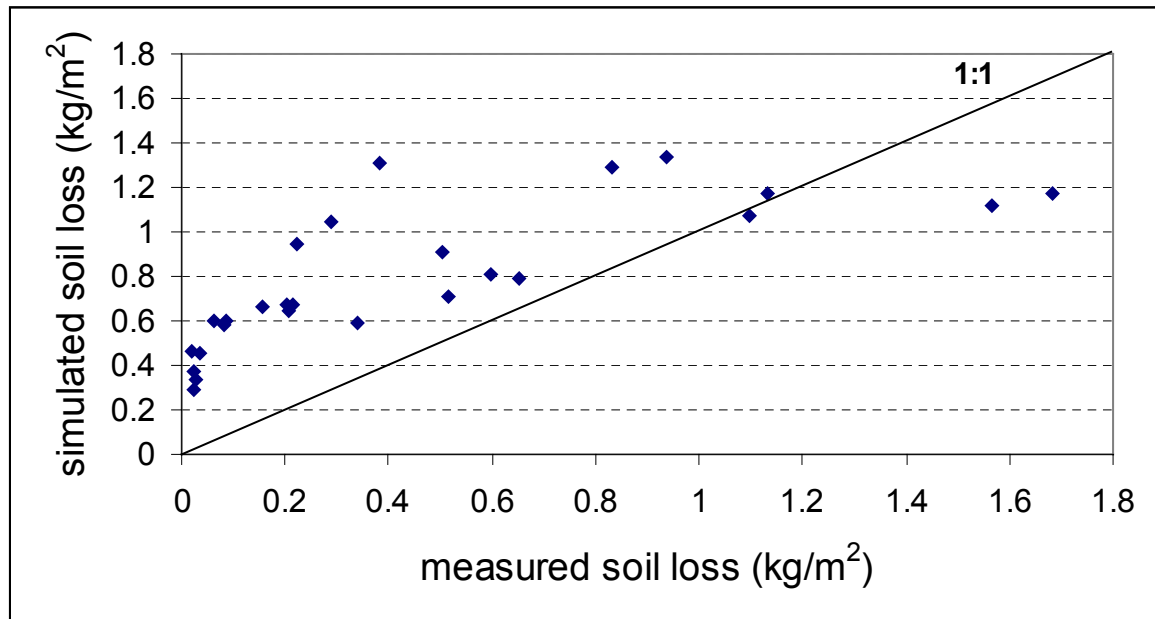


A similar evaluation was done for the MMF model. This resulted in the equation

$$\text{Soil loss (MMF)} = 1.098 (\pm 0.28) * \text{measured soil loss} \quad (n = 26, r = 0.85) \quad (8)$$

Figure 16 gives a visual impression of this relationship. A comparison between measured soil erosion values and MMF gives a correlation coefficient of 0.71 and a mean standard error for the prediction of soil erosion yields of 0.13 for MMF. This result implicates that for the MMF model application the erosion value cannot be estimated with a higher precision than ± 0.52 (95% probability). Equation 3 reveals an overestimation of erosion for lower erosion amounts, while larger erosion rates are underestimated. Compared to the relationships for the USLE and the MUSLE, this relationship exhibits a lower degree of uncertainty. Only for the cases with low erosion rates up to 0.5 kg/m² a considerable overestimation of simulated soil loss can be observed.

Figure 16: Comparison of measured erosion data obtained via rainfall simulation experiments with calculated erosion data using the MMF equation.



2.3.2 Calibration of erosion models at subbasin level

As a basis for calculation and calibration of surface runoff the knowledge of the regional water balance is essential. Water balance calculations for the Ybbs and the Wulka river basin have been carried out by IHGW (2003) using the water balance model Difga2000 (Schwarze, 2001). This enabled to separate total flow into slow groundwater flow, fast groundwater flow and direct flow. Direct flow rates of Difga2000 were then used for calibration of runoff for both soil erosion models. The drainage basins of the river Ybbs and Wulka were divided into several subbasins. These were used for calibration. In addition river basin outlet data were used to validate calibrated results. Hydrologic calibration for the SWAT model was performed by IHGW (Deliverable D1.1.).

Ybbs

Table 10 gives the calibration results for SWAT and MMF. Concerning the mean flow conditions predicted by the SWAT model an overprediction of most of the subbasins can be stated. Reason for this is an insufficient modelling of runoff events caused mainly by the lateral flow of the faster groundwater runoff (Deliverable D 1.1). Compared to mean flow conditions, low flow and high flow conditions are reproduced better. Further details of the calibration for SWAT are described in Deliverable D 1.1.

Table 5: Runoff calibration results for the different subbasins (north to south) and the main outlet of the river Ybbs, average percentage of total river discharge; simulation period 1991-1997

Surface Runoff (%)	Main outlet	Subbasins			
		Krenstetten arable land	Ybbsitz grassland	Opponitz forested	Lunz/Ois forested
Baseflow seperation Difga	28.6	32.5	22.9	29.4	31.2
Soil erosion model MMF	32.0	32.5	22.4	29.4	31.5
Soil erosion model SWAT	37.0	56.0	39.0	37.0	23.0

Main parameter for calibrating the MMF model was the parameter “effective hydrological depth” which is suggested by Morgan (2001) whenever measured runoff data are available since there are problems in describing this parameter. This parameter is a surrogate for the amount of water which may be stored in a soil before runoff starts. The correlation coefficient between measured and predicted data for MMF is 0.93 which indicates that the model is able to be reasonably well calibrated for surface runoff in this area. Especially, the different land use management in the subareas is represented well (Table 5). However, mean surface flow at the Ybbs basin outlet is overpredicted. Table 6 gives a comparison of parameter values for effective hydrological depth proposed in the original paper and those obtained after calibration. These values differ hugely. The Ybbs river basin is characterised by a strong gradient in climate, landuse, slope and geomorphology from south to north. Water flow follows this pattern. Therefore, the southern parts of the basin, which may be already characterised as alpine areas exhibit high water flow rates but the land is almost exclusively covered with forest or grassland. Direct flow rates given by Difga2000 also include the quick subsurface flow in the unsaturated zone and this flow path is of especial importance for alpine areas with high slopes and shallow soils. On the other hand, MMF deals only with surface runoff leading to an incompatibility between model structures. However, the consequences of these high “surface” flow rates for erosion estimation are less than expected due to the dense ground cover of these areas which reduced erosion enormously.

Table 6: Calibration Parameter for MMF „effective hydrological depth“

Vegetation	Values given by Morgan (2000) (m)	Calibrated Values (m)	
		Ybbs	Wulka
Row crops	0.12	0.45	0.25
Mature forest	0.20	0.02	0.4
Cultivated grass	0.12	0.024	0.4
Vine	0.14	-	0.6

Wulka

After calibration MMF again is able to describe the regional water balance of the Wulka catchment appropriately. This is also confirmed by a correlation coefficient of 0.96 between measured and calculated runoff values. Table 7 reveals a tendency to overpredict surface runoff except in the subbasin Walbersdorf which is the only more hilly region dominated by forest in the catchment. The subbasin Walbersdorf is not as mountainous as the origin of the river Ybbs and as forest is also situated in lower areas it was not possible to diminish the parameter.

Table 7: Runoff calibration results for the different subbasins and the main outlet of the river Wulka percentage of total river discharge; simulation period 1992 - 1997

	Main Outlet	Subbasin			
		Walbersdorf	Wulkaprodersdorf	Oslip	Nodbach
Difga	17.6	18.0	19.6	23.7	26.3
MMF	22.1	17.3	23.3	29.9	40.0
SWAT	40.0	48.0	21.0	27.0	16.0

Table 6 gives the values for the calibration parameter obtained after calibration for the subbasins in the Wulka catchment. The direction of the calibration changed compared to the Ybbs catchment. This suggests that the runoff algorithm which is implemented in the MMF model is strongly influenced by the climatic situation of a catchment in general. While the values given by Morgan (2001) may represent some kind of means, the Ybbs river catchment with high flow conditions needs a decrease in “effective hydrologic depth” which leads to increased surface runoff generation. The Wulka river exhibits much lower surface runoff rates due to the general climatic

situation in this area. This in turn is reflected in higher values for effective hydrological depth compared with the table values suggested by Morgan (2001). In addition mountainous regions with very shallow soils and steep slopes deliver most of the rain as surface runoff or near surface runoff while comparably flat areas such as the Wulka catchment infiltrate much more water. This can also be seen in the north of the Ybbs catchment where the parameter for row crops had to be increased to fit runoff.

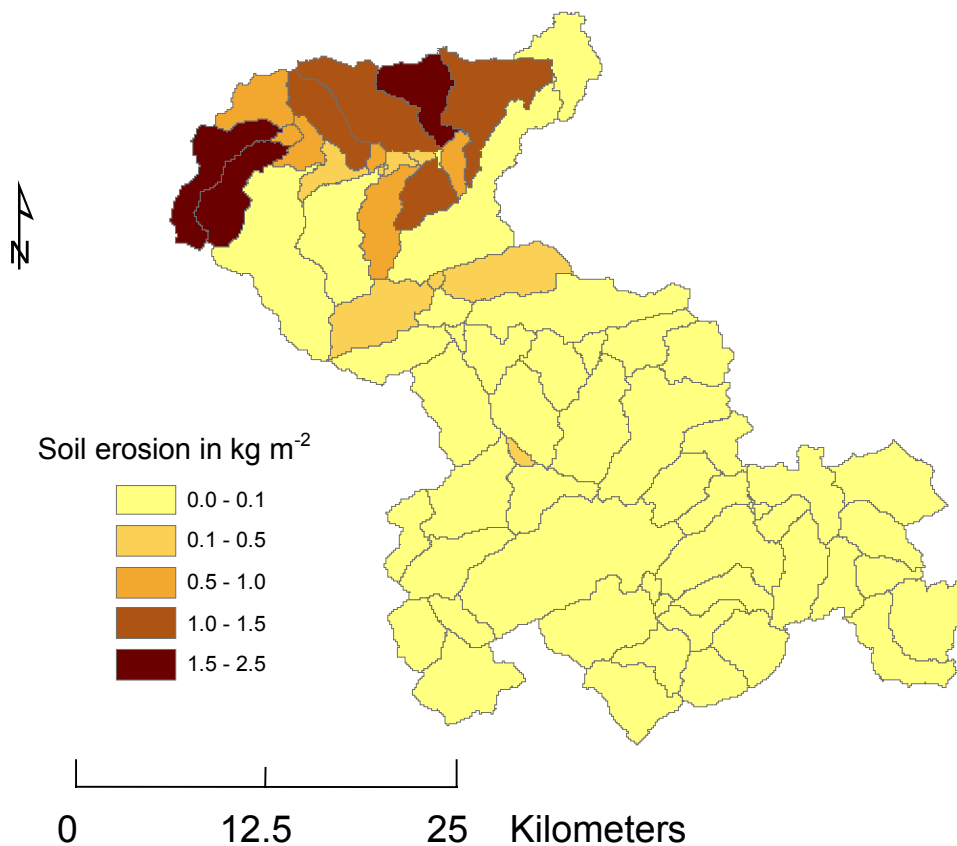
2.4 Simulated sediment loads

2.4.1 Ybbs

MUSLE

Simulation of sediment loads using the MUSLE approach was completely done within SWAT. Basis for the simulation were the calibrated water flow components (for a discussion of problems see Deliverable 1.1). Consequently we used identical evaluation periods for our model application. Figure 17 gives the spatial distribution of sediment yield for the Ybbs river catchment on the basis of subwatersheds. According to the SWAT handbook (Neitsch et al., 2001) simulated sediment yield should be comparable to measured values once the water balance calibration was done. We did, therefore, not include any instream calculations to handle sediment routing or deposition in the stream but compared only the sediment load which was transported into the stream. This is equal to the assumption, that all sediment which reaches the stream also leaves the watershed. We also did not account for stream bank erosion, which, under specific circumstances may contribute considerably to the total sediment production of a river (DeRose et al., 2002). However, riparian cover, the most important control factor for riverbank erosion, is quite dense for the Ybbs as well as the Wulka river catchments. Therefore we deem riverbank erosion for our environments to be low compared to soil erosion.

Figure 17: Simulated sediment yield (t/ha/a) for various subcatchments of the Ybbs river catchment using the MUSLE approach of SWAT



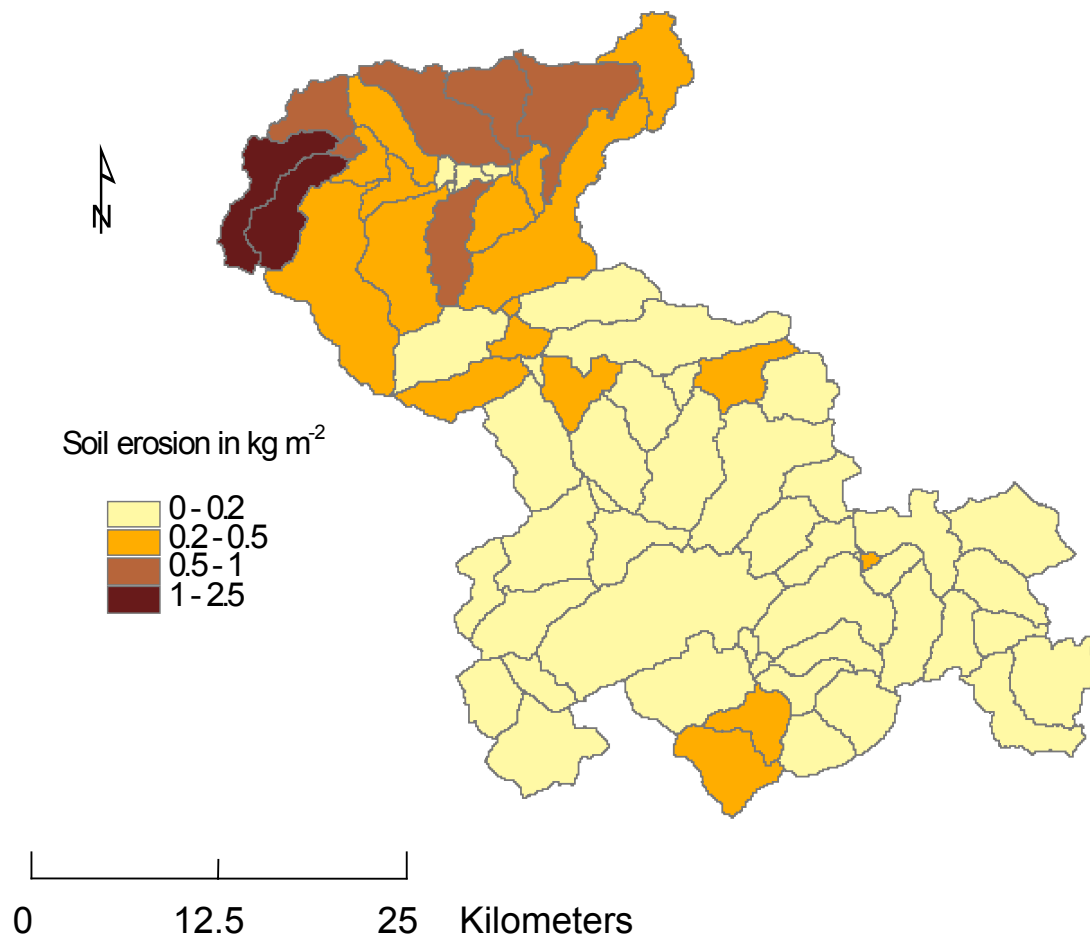
MMF

Differently to SWAT, runoff and soil erosion were calculated for individual grids (see model description). For ease of comparison, results of MMF were averaged on the same subbasin level (73 subbasins) as used by SWAT. Similarly to our SWAT calculations we assumed no changes of sediment yield as soon as soil erosion has delivered into the stream. This assumption is supported by the fact, that field inspection in the Ybbs river basin did not confirm big amounts of retention, main channel processes were not calculated. To compare results, we used the same simulation periods as for the modelling in SWAT (1991-97).

Sediment yield in the river Ybbs was calibrated against measured values at the stations Opponitz and Krenstetten. These two stations reflect very well the different environmental situations within the study catchment. Calibration was done only to that point, where data values for calibrated parameters were still in the range of reported values. Measured results at station Greimpersdorf (basin outlet) were finally

compared (no calibration at this station) to results simulated with MMF. Figure 18 gives the areal extension of the simulated soil losses for the various subcatchments of the Ybbs river.

Figure 18: Simulated sediment yield (t/ha/a) for various subcatchments of the Ybbs river catchment using the MMF model

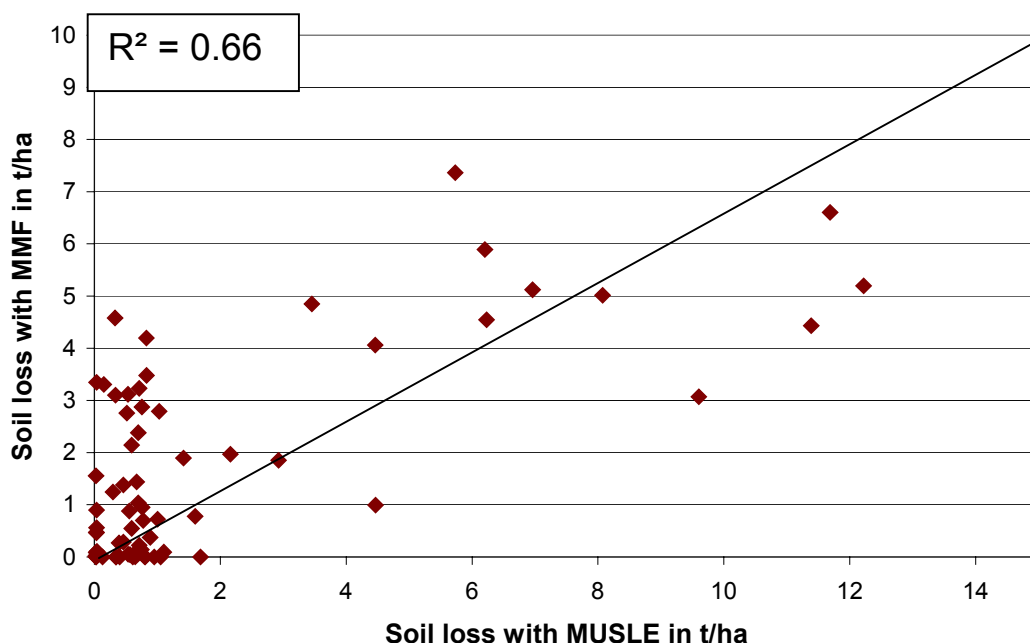


Model Comparison and comparison of simulated and measured sediment loads

A comparison of areas affected by erosion gives a relatively good agreement between results calculated with MUSLE and those obtained with MMF. The results of this comparison of MMF and MUSLE for the period 1991-1997 (Figure 17) indicate a general agreement on soil loss risk estimation. Results of both models reflect the landuse pattern with low erosion rates in the alpine areas and higher erosion rates in areas with more intense agricultural landuse. However absolute values of soil loss differ considerably. One reason for this are the different structures of MMF and MUSLE models. While the MUSLE concept in the SWAT system uses only one input

value for each parameter to calculate erosion for a hydrological response unit, the MMF model calculates erosion on a grid basis (25 m²). Within one subbasin a lot of grid cells exist, which do not have any erosion (such as pasture, forests but also agricultural areas with low erosion rates such as footslopes or basin areas). Anyway, they are all included in the mean value/subbasin calculations for MMF. Figure 19 demonstrates the general agreement in calculated soil losses for both models for higher calculated soil losses. However, SWAT exhibits a tendency to estimate higher soil losses compared to MMF for those subbasins with a higher soil loss risk. This can be confirmed by the slope value of the linear regression between results of both models which is 0.6 (1 indicates perfect agreement). This compares well with results for the USLE that demonstrate a general overestimation of model predictions at higher soil loss risks (Risse et al., 1993; Strauss and Klaghofer, in press). For particular subbasins, considerable variation in results between the models occurs. For areas with low erosion rates calculated by SWAT and higher erosion rates calculated by MMF, this may be explained by the fact, that SWAT calculates single input values for each HRU or subbasin. In heterogeneous areas with very different landuse intensities SWAT uses those landuse parameters with the greatest areal extension. Therefore, small areas with a high erosion risk may be neglected, whereas MMF uses all grid values of a subbasin for calculation of average soil loss.

Figure 19: Relationship of soil loss calculated with MUSLE as compared to soil loss calculated with MMF (both in kg m⁻²) at subbasin level



For particular subbasins, considerable variation in results between the models occurs. For areas with low erosion rates calculated by SWAT and higher erosion rates calculated by MMF, this may be explained by the fact, that SWAT calculates single input values for each subbasin. In heterogeneous areas with very different landuse intensities SWAT uses those landuse parameters with the greatest areal extension. Therefore, small areas with a high erosion risk may be neglected, whereas MMF uses all grid values of a subbasin for calculation of average soil loss.

A further step of model comparison was to calculate sediment concentrations by dividing soil loss of the different subbasins by calculated surface runoff. This resulted in a better correlation between the models ($R^2 = 0.71$). In addition, the slope value of the regression between MMF and SWAT was not different from 1, indicating that both models react in the same way.

Model results may also be compared to measured data at those locations, where monitoring had taken place. Procedures to calculate sediment loads are presented in Deliverable D 1.3. A comparison of calculated versus measured loads at the three stations where a detailed monitoring programme had taken place (Table 8) reveals that calculated sediment loads for station Opponitz have the best agreement for both models. The relatively high yield in this forested mountainous area is caused by very steep slopes (average more than 30°). MUSLE overpredicts sediment loads for the other stations hugely, while MMF overpredicts only for station Krenstetten. The better fit of MMF to measured data is not surprising as for the MMF also sediment load had been calibrated (at stations Opponitz and Krenstetten). The fact that even with a calibration of MMF at Krenstetten no better fit could be done indicates, that with a further calibration unrealistic input data would have been necessary. The overpredictions of sediment load with MUSLE indicate, that the assumptions of the model that no further inclusion of a sediment delivery ratio is necessary due to inclusion of an explicit runoff term, do not hold. According to this assumption, the huge differences between measured and calculated loads could only be explained by retention in the river itself. However, field inspection in the Ybbs river basin did not confirm such big amounts of retention. We therefore conclude, that redistribution of soil inside the subbasins constitutes the majority amount of soil erosion. This is confirmed by work of Martínez-Casnovas et al. (2001) who found a soil loss

retention of more than 50 % already at the field scale and Strauss and Peinsitt (2002) who mapped soil redistribution rates of a small basin of more than 800 t compared to sediment losses of about 20 t leaving the same watershed.

In addition, a calibration of soil loss is not really possible because the treatment of some model parameters in the SWAT system remains unclear (e.g. slope factor, mean C-factor). We did some additional testing of the sediment routing routine within SWAT. This routine calculates sediment loads by taking water flow in the river into account. This reduces the sediment load considerably. Anyway, we could not manage to check the processes and equations taken into account completely because of unclear descriptions in the SWAT manual.

Table 8: Comparison of calculated MUSLE and MMF (already calibrated) values and measured sediment load at the stations Opponitz, Krenstetten and Greimpersdorf (mean values for the years 91-97)

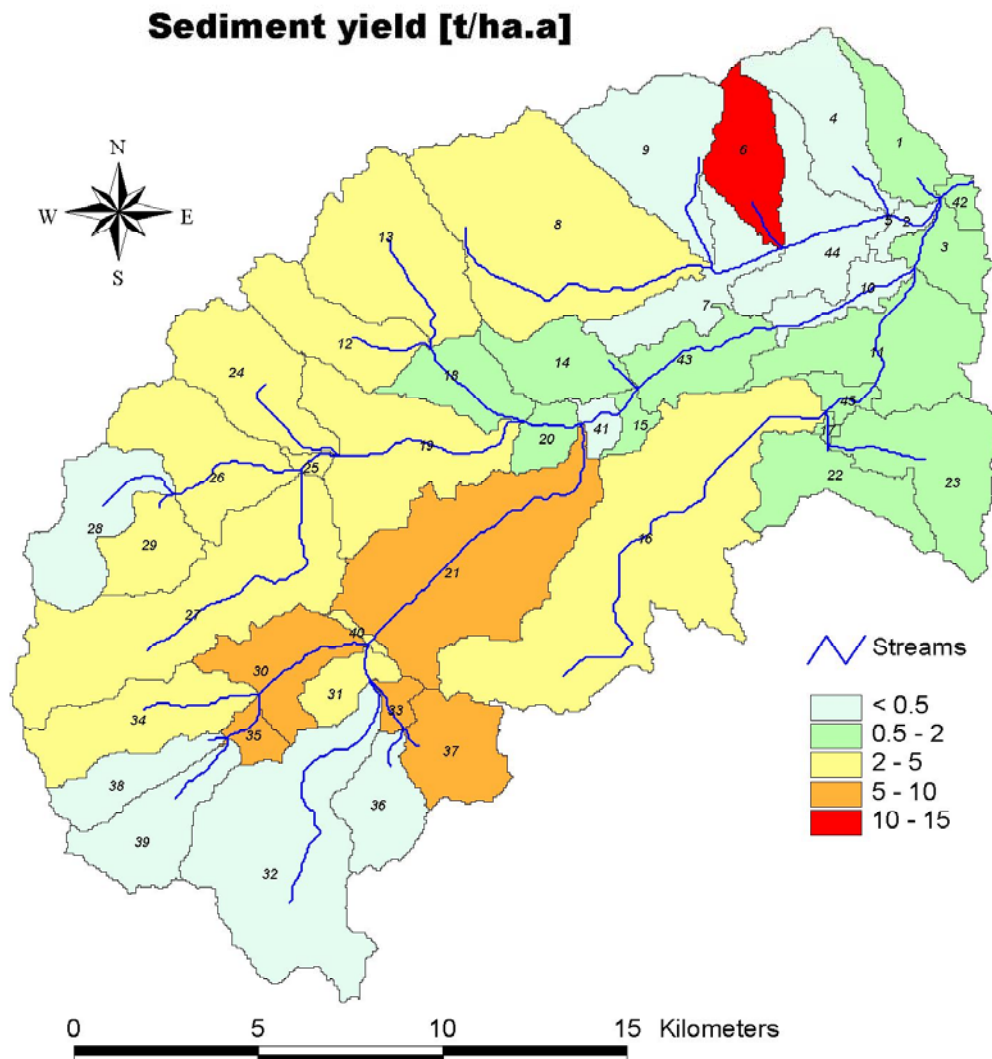
Station	Sediment load (t/ha/a)		
	Calculated - MMF	Calculated - MUSLE	Measured
Opponitz	0.4	0.5	0.4
Krenstetten	1.0	6.2	0.4
Greimpersdorf	0.7	2.7	0.7

2.4.2 Wulka

MUSLE

Figure 20 gives the spatial distribution of calculated sediment yield for the Wulka river catchment on the basis of 45 subwatersheds. Compared to calculated sediment loads for the Ybbs river, these values are in general lower. Also, no big spatial differences are to be observed. Although landuse is mostly dominated by arable land owing to flat slopes and low precipitation soil erosion is not high. Mean precipitation is almost half of Ybbs catchment. Whenever slopes increase over 10 (in the south and in the north) landuse changes into forest.

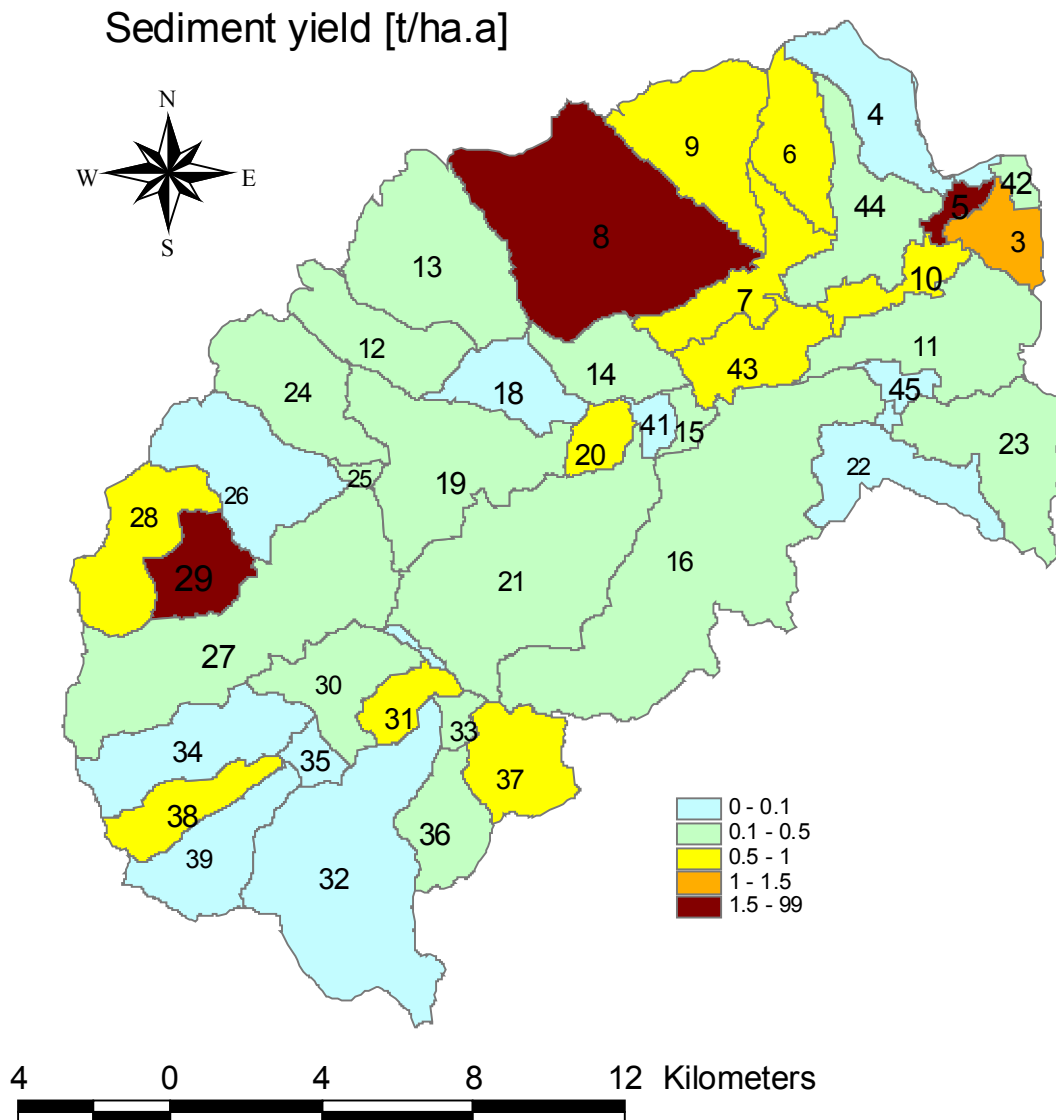
Figure 20: Simulated sediment yield (t/ha/a) for various subcatchments of the Wulka river catchment using the MUSLE approach of SWAT



MMF

A simulation for the Wulka catchment was also done using the MMF model. As already discussed above, to make the models comparable, results of MMF were averaged on the same subbasin level (45 subbasins) as used by SWAT.

Figure 21: Simulated sediment yield (t/ha.a) for various subcatchments of the Wulka river catchment using the MMF model



Comparison simulated – measured sediment loads

Comparing simulated with observed sediment loads a similar tendency as compared to the Ybbs river catchment can be observed. Again, simulated sediment load of SWAT is about an order of magnitude higher compared to measured values (Table 9). Compared to the Ybbs river, the different subwatersheds do not differ very much in terms of land use and general environmental conditions. This may be seen very well at the similar sediment loads of the different measurement points in the watershed. This result is also reproduced by the MUSLE. It can be concluded, that a subdivision of this kind of watershed into smaller units is not necessary.

The spatial pattern of soil erosion in the two models is similar. Higher soil erosion occurs in subbasins dominated by vineyards and low erosion in forested areas in the south.

Table 9: Comparison of calculated MUSLE and MMF (already calibrated) values and simulated sediment loads for different subwatersheds of the Wulka river catchment (mean values of the years 92-97)

Station	Sediment load (t/ha/a)		
	Calculated - MMF	Calculated - MUSLE	Measured
Walbersdorf	0.2	1.9	0.2
Wulkaprodersdorf	0.2	2.9	0.2
Schuetzen	0.4	2.4	0.2
Trausdorf	0.3	2.8	0.2
Oslip-Eisbach	1.0	2.1	0.1
Nodbach	0.2	2.0	0.1

As the water flows down the different subcatchments, water flow and sediment load are supposed to increase. These results are calculated sediment loads by MMF. However, measured loads at the different subbasins do not follow this pattern, which is surprising. The results of the two erosion models can not be compared directly due to the fact that in contrast to MUSLE, results of sediments in MMF model have been calibrated and therefore are quite similar to measured data with the exception of subwatershed Oslip. We tried to find reasons for this behaviour. However, runoff rates fit very well and landuse is not really different to other subbasins. In addition, drainage density which could strongly influence sediment yield in the MMF model is similar to other subbasins. So at the moment we are not able to explain this behaviour. In addition it appears that the measured loads at Oslip are quite low.

2.5 Simulated phosphorus loads

With increasing contribution of soil erosion out of agricultural land, the importance of this pathway to phosphorus inputs into aquatic ecosystems increases. Therefore accurate prediction of sediment delivery is an important and effective approach to

predict phosphorus discharge into river systems. We calculated phosphorus loads for the various monitoring points of the river Ybbs and Wulka and compared these values to phosphorus loads calculated with two different algorithms connected to the different erosion models. Phosphorus concentrations to be used for the load estimation were calculated as total phosphorus (mg/l) minus total phosphorus of the filtered sample (mg/l). The subsequent calculations therefore correspond to the phosphorus load which is attached to sediment > 0.45 μm .

MUSLE

To simulate total phosphorus loads for the Ybbs and the Wulka river catchments using the MUSLE results as a basis, as a first approach the algorithms implemented in the SWAT interface were used. Main task was to simulate particulate phosphorus as this is attached to erosion. Nevertheless future efforts should also consider dissolved P for two reasons: a) at least in agriculturally used areas dissolved P loads makes up to 20% of the total load and b) whereas particulate P loads may or may not contribute to eutrophication processes immediately, dissolved P is very likely to do so.

Loading of total P is calculated with basically three equations (Neitsch et al., 2001):

$$\text{SedP} = 0.001 \cdot \text{conc}_{\text{sedP}} \cdot \frac{\text{sed}}{\text{area}} \cdot e \quad (9)$$

$$e = 0.78 \cdot (\text{conc}_{\text{sed}})^{-0.2468} \quad (10)$$

$$\text{conc}_{\text{sed}} = \frac{\text{sed}}{10 \cdot \text{area} \cdot Q} \quad (11)$$

where SedP = amount of P transported with sediment (kg/ha)

$\text{conc}_{\text{sedP}}$ = concentration of P in the top 10 mm of soil

sed = sediment yield on a given day (t)

area = area of hydrological response unit (ha)

e = P enrichment ratio

conc_{sed} = concentration of sediment in surface runoff (t sediment/m³ water)

Q = surface runoff (mm)

All calculations were performed with the settings that had been obtained after preceding calibration procedures. To calculate P content of the topsoil, the default

settings proposed by SWAT were used in a first attempt. For this test we did not include any fertilisation to check the system response to such assumptions. In a second set we changed the default values and added fertiliser every year to an amount of 40 kg P/ha as mineral fertiliser and 10 kg P/ha as organic fertiliser to all crops for the Ybbs river and 50 kg P/ha as mineral fertiliser for the Wulka river. Grassland received only organic fertiliser to an amount which corresponds to the mean GVE/ha for the respective catchment (1.5 GVE/ha for the Ybbs river catchment and no organic P for the Wulka river according to the data of Agrarstrukturhebung 1999). To account for fertilisation of grassland in the Wulka river, inorganic fertiliser was added to an amount of 30 kg P/ha each year. For the default settings, a basic content of 5 ppm labile P is suggested and the amount of organic P is calculated according to fixed relationships given in the SWAT user manual. No explanation is given directly to which kind of extraction procedure the values of labile and organic P refer. Anyway, the algorithms implemented in SWAT have been developed by Jones et al. (1984). Sharpley et al., (1984) have derived equations to predict amount of labile P from various other extraction methods. Unfortunately, data for none of them are usually available in Austria. To check the appropriate amount of initial labile P we therefore took soil values, which had been measured in another European project (DESPRAL). There, the respective values for labile P had been measured for three Austrian soils (Interrim report of the DESPRAL project, unpublished data). A typical value for labile P content for these soils was in the range of 10 –20 ppm P (Olsen extraction procedure). With these values and an equation to translate into labile P (Sharpley, 1984) we assumed a mean amount of labile P for all intensively used agricultural areas of 15 mg P/kg soil for the Ybbs catchment. Water quality data for the Wulka catchment indicate, that the basic level of labile P is higher. To account for this we assumed a value of 25 mg P/kg soil (according to the SWAT user manual this is a typical value for agriculturally used land). As no data exist to give initial values for organic P, the relationships given in the SWAT user manual had to be assumed for both catchments.

According to the results obtained for sediment loads, evaluations were done for the same period of 1992 –1997. Given values are means for that period.

Ybbs

Table 10 gives a comparison of total P concentrations of the sediment, as obtained with SWAT simulations for various years and two different test situations. For test situation 1, only default values suggested by SWAT were taken and no fertilisation was applied. As a consequence, mean levels of total P in sediment decline very rapidly. Although logical in a long term perspective, such kind of reaction is not to be observed usually in the short term as also indicated by recent results of long term P applications in a nearby experimental plot (Spiegel et al., 2001). To maintain constant P levels in the sediment it is therefore necessary to add fertiliser. Another possibility might be to change parameters (for instance the P availability index) in the phosphorus cycling component of SWAT but this needs information about probable values for the different parameters proposed, which to date is not available. In a second test we therefore added fertiliser to the systems (as described above) and changed the initial values for labile soil P content to get realistic assumptions. This stabilised the annual fluctuations and doubled the content of P in the sediment. Anyway, compared to the measured median values, given in Deliverable D 1.3. (loading calculations) of 1367 mg P/kg sediment at station Greimpersdorf, the median of 890 mg P/kg sediment is about 30 % lower. The only way to change this would be to either increase the level of P in the soil and also increase fertilisation, or change the relations between soil erosion and P transport i.e. enrichment ratio. In the case of higher initial P levels and higher fertilisation rates, measured (at least to some extent) data are in contradiction to this.

Table 10: Mean total P contents of sediment (mg P/kg sediment) for selected subbasins as simulated with SWAT for different years: test 1 = only initial defaults values and no fertiliser added; test 2 = initial P level given plus annual fertiliser

Year	TOTAL	Subwatershed 3		Subwatershed 1		Subwatershed 6	
		Test 1	Test 2	Test 1	Test 2	Test 1	Test 2
1991	936	320	683	334	644	504	783
1992	1000	290	785	308	714	507	894
1993	956	256	788	299	703	415	737
1994	982	178	783	252	681	389	740
1995	928	225	854	289	698	396	714
1996	843	175	661	234	598	322	650
1997	771	157	674	216	578	298	592
Mean	892	247	769	286	656	422	731

Table 11 gives a comparison of measured and simulated P loads for different subwatersheds of the Ybbs river. Simulated P loads are given as sum of inorganic and organic P attached to sediment.

Table 11: Calculated MUSLE (SWAT) and measured total P loads for the Ybbs river watershed (period 91-97)

Station	P load (kg/ha/a)	
	Simulated	Measured
Opponitz	0.3	0.3
Krenstetten	2.0	0.5
Greimpersdorf	0.9	0.7

A comparison between measured and simulated P loads reveals a good agreement for stations Greimpersdorf and Opponitz and an overprediction of simulated P loads for station Krenstetten. This reflects very well the situation of sediment prediction. There, the deviations between measured and simulated P loads are smaller due to the underprediction of P concentration in the sediment. In fact, this leads to the result,

that for station Greimpersdorf, measured and predicted P loads are quite close (correct results for the wrong reason).

Wulka

Similarly to the methodology applied for the Ybbs river catchment, P loads for the Wulka river catchment have been calculated.

Table 12 compares results of calculations with measured data. Again, the overprediction in sediment yield is the main reason for overprediction of P load.

Table 12: Calculated MUSLE and measured total P loads for the Wulka river watershed (period 1992-97)

Station	P load (kg/ha/a)	
	Calculated	Measured
Walbersdorf	0.7	0.4
Wulkaprodersdorf	1.2	0.3
Schuetzen	1.0	0.5
Trausdorf	1.2	0.3
Oslip-Eisbach	0.8	0.3
Nodbach	0.9	0.2

MMF

Phosphorous loads were also calculated within the MMF Model approach. To do so, an additional algorithm governing movement of phosphorus attached to soil particles from land areas to the stream network was implemented in the model structure.

Eroded sediments usually contain much higher sediment-bound P compared to the topsoil in the upland source area (Sharpley, 1984). The higher phosphorous content in the sediments is due to selective processes of erosion and transportation of fine sized particles. Sediment discharge is enriched by clay particles. Furthermore phosphor in the soil is preferentially attached to colloidal particles. Phosphorous enrichment ratios are used to take this into account, to quantify the increase in particulate P in the eroded sediment compared to that in the upland area topsoil.

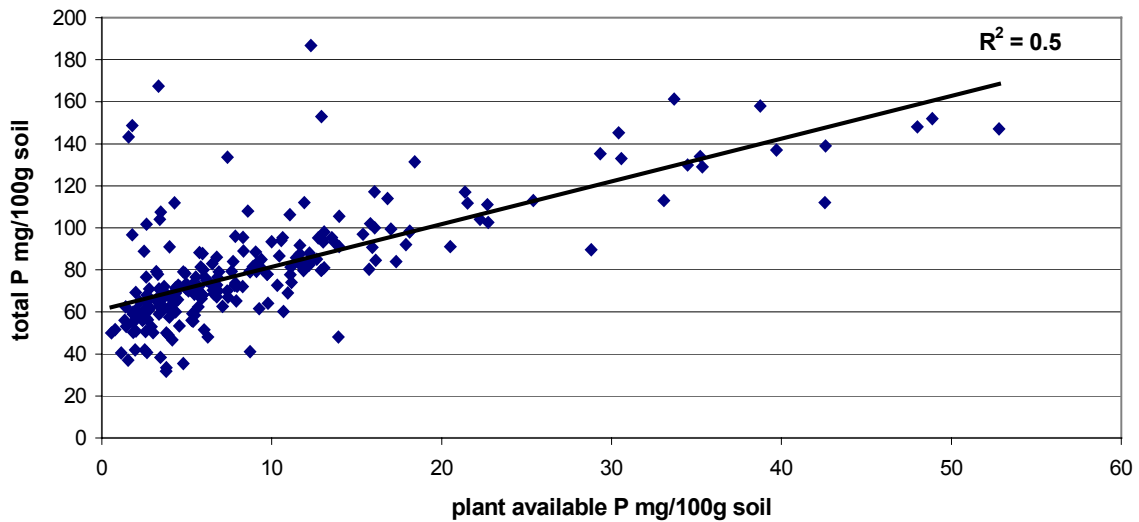
No values of total phosphorus nor any kind of labile phosphorus fraction for the topsoil is available to cover the tested case study areas completely. No Austrian monitoring system for soil information covers this parameter (Schwarz et al., 2001a). For the northern part of the Ybbs catchment (Amstetten) some values for plant available phosphorus (measured as CAL- P in Austria and some other European countries, see ÖNORM L 1087, 1993) and total P have been measured (KS Bodenuntersuchung Amstetten, data submitted by IWQ of TU Vienna). These data were assumed to be representative for the region. For the areas not covered by the data some measurements on plant available P exist (given by AGES). It was therefore necessary to calculate a relationship between plant available and total P amounts. Two additional data sets were used for this. Values for plant available P (measured in CAL) and total P had been measured within another European project (DESPRAL) and also within a project carried out by BOKU (data given by Institute for Soil Science). All these data have been pooled and used to develop the relationship given in Figure 22. As a variety of different European soils are covered in this data set, it could be used for other regions as well. However, one European problem in that sense is, that many different methods are used to describe plant available P in the different countries.

$$TP = 2.0338 * IP + 61.07 \quad r^2 = 0.5, n = 232 \quad (12)$$

where: TP = total P content in the topsoil in mg/100g

IP = plant available P content measured as CAL-P in mg/100g

Figure 22: Relationship between measured total P and labile P (measured in CAL) loads for different soil types.



This relationship was used to obtain total P contents for agriculturally used land in both case study areas at the level of communities. Values for forested areas were obtained from the Austrian soil monitoring system for the federal provinces of Burgenland and Lower Austria (Bundesanstalt für Bodenkultur, 1994, Bundesamt und Forschungszentrum für Landwirtschaft, 1996) via the BORIS data base of the Umweltbundesamt (Schwarz et al., 2001b).

Table 13 gives mean values for phosphorus concentrations of the different landuse units in the case study areas. Figure 23 and Figure 24 give a visual impression on the spatial distribution of total phosphorus in the case study areas.

Figure 23: Distribution of total phosphorus in soil in the Ybbs river basin

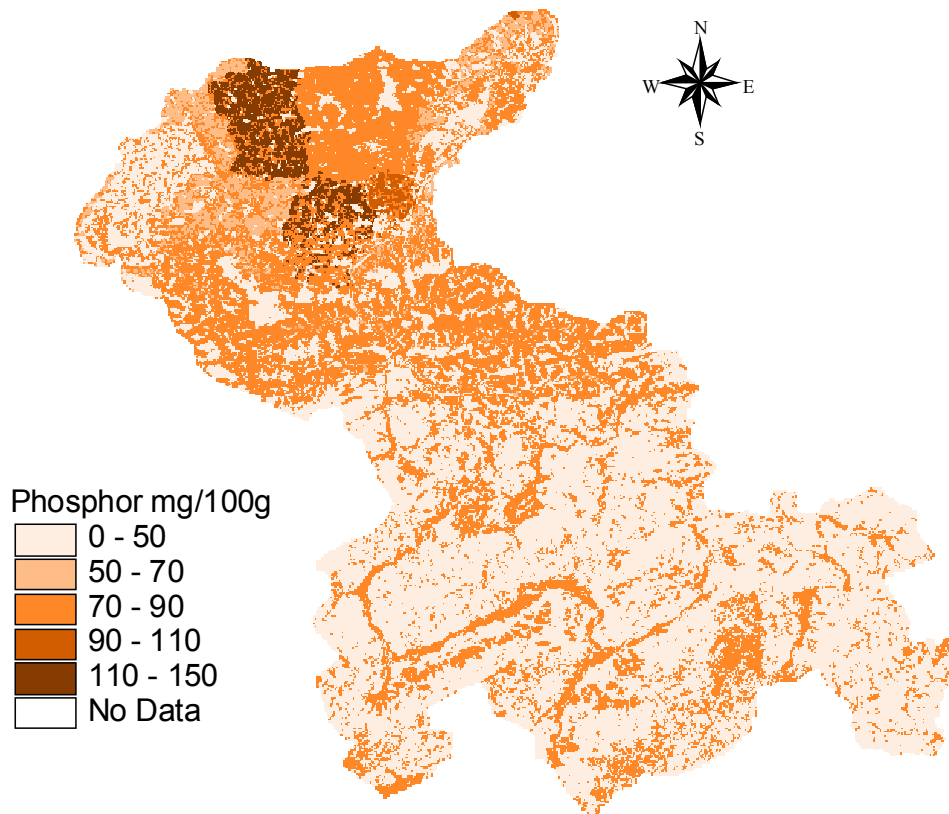


Figure 24: Distribution of total phosphorus in soil in the Wulka river basin

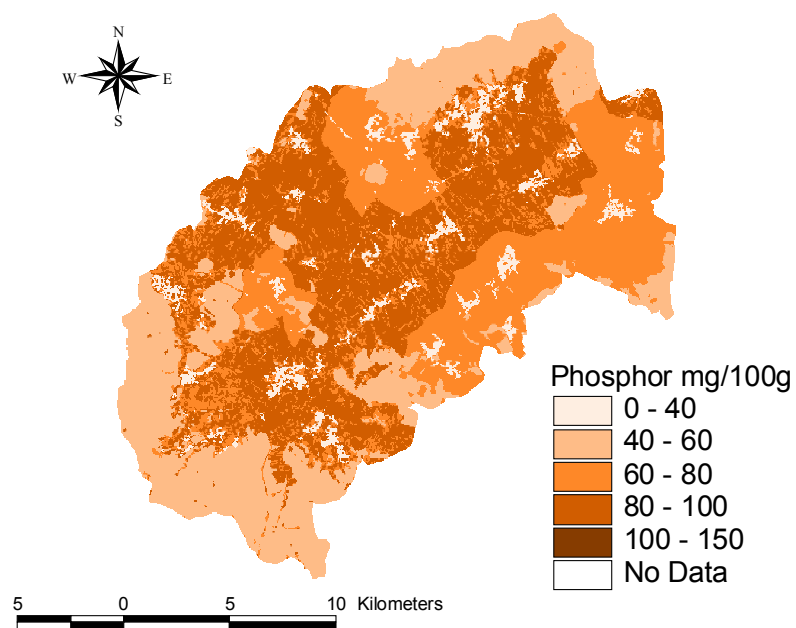


Table 13: Mean concentrations of total phosphorus for different landuse units in the case study areas

Total phosphorus (ppm)				
Landuse	n	Mean*	Median	Standard deviation
Forest –Wulka	77	506	480	257
Forest Ybbs	445	475	430	283
Arable – Wulka	2255	811	-	-
Arable – Ybbs	7691	732	-	-
Pasture – Wulka	2255	811	-	-
Pasture - Ybbs	7691	732	-	-

*calculated according to equation 7).

To take the differences between total P content in the topsoil and the P content in the river sediment into account enrichment ratios were calculated as the concentration of total P in the simulated sediment divided by that in the soil for each subbasin. Obtained enrichment ratios were then averaged for each case study area.

$$E = \frac{\text{SEDP}}{P_{\text{soil}} \times \text{SED}} \times 10^6 \quad (13)$$

Where E = P enrichment ratio

SEDP = measured amount of P transported with sediment (kg/a)

P_{soil} = amount of total P in the topsoil (mg P/kg)

SED = simulated sediment load (kg)

Obtained mean enrichment ratios for the two case study areas were 1.2 ($s_x = 0.97$) for the Wulka river and 1.0 ($s_x = 0.40$) for the Ybbs river. The standard deviations of these values are given in parentheses. They indicate considerable variation for the different subbasins.

Table 14 gives a comparison of measured and simulated P loads for different subwatersheds of the Ybbs and the Wulka river.

Table 14: Calculated MMF and measured total P loads for the Ybbs and the Wulka river watershed

Station	P load (kg/ha.a)	
	Calculated MMF	Measured
<u>Ybbs:</u>		
Greimpersdorf	0.5	0.7
Krenstetten	0.6	0.5
Opponitz	0.4	0.3
<u>Wulka:</u>		
Schuetzen	0.5	0.5
Walbersdorf	0.2	0.4
Wulkaprodersdorf	0.3	0.3
Trausdorf	0.3	0.3
Oslip-Eisbach	1.5	0.3
Nodbach	0.4	0.2

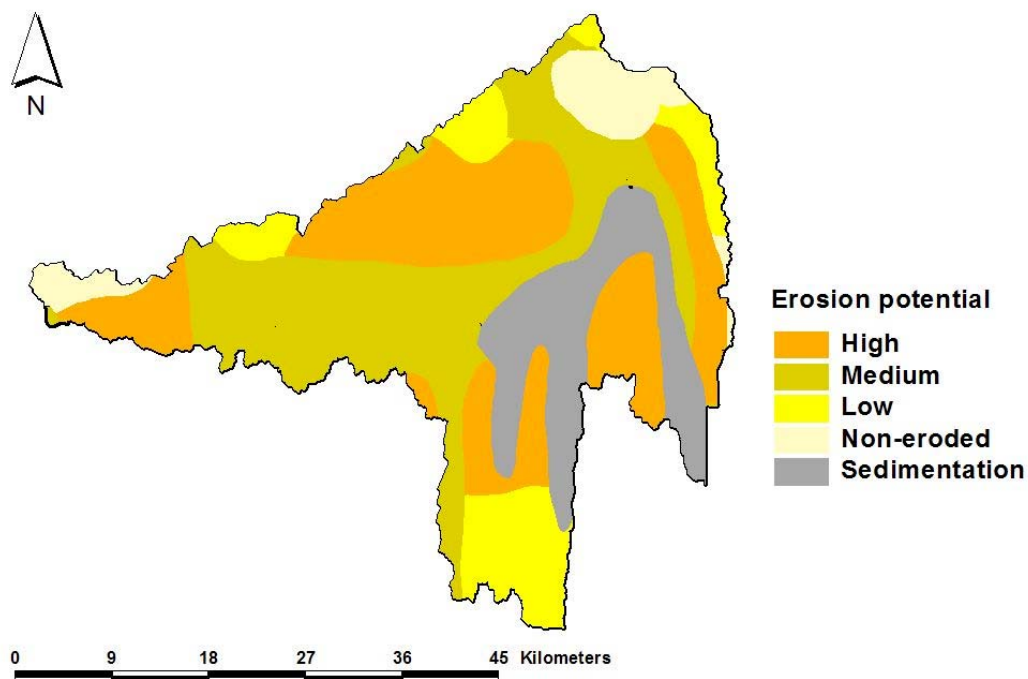
Analysis of the individual gauging stations shows that the subwatersheds of the Ybbs river are in general predicted better compared to the Wulka river subbasins. The high overprediction in the subcatchment Oslip may be explained by a high overprediction in the simulation of the sediment yield in the river. Similar considerations hold for the subbasin Nodbach, where the simulated sediment yield was twice the measured one. The situation at station Walbersdorf is different. Here the simulated sediment yield compared well to the measured results. Therefore, the underprediction of simulated P loads has to be attributed to a failure in describing P loading.

3 THE ZALA RIVER CASE STUDY

The Zala River catchment is very sensitive to soil erosion. A study, made in 1996 (Agrober Ltd., 1996), reported that the average soil loss rate of the watershed was approximately 10 t/ha/year. That means a total soil loss of nearly 1.500.000 t/year. However, the measured sediment load in the river at the catchment outlet was 5.000-15.000 t/year in the 90ies. The large difference between the two values is the amount of eroded soil which does not get out of the watershed. The erosive potential of the area is shown in Figure 25. This chapter presents the process of sediment input calculation into the river and its comparison to the measured loads. The determination of this sediment input is very important for the phosphorus load simulation, because the majority of non-point source phosphorus pollution is bounded to the soil particles. The simulation method is the MUSLE model (Williams, 1982) described above, which is incorporated into an integrated watershed model in GIS environment called SWAT model (Arnold et al., 2000). Since surface runoff has already been determined with the calibrated hydrological sub-model of SWAT (see Water Balance Report of the Project), this input of the MUSLE model is not detailed here. The following sub-chapters contain descriptions about the soil database development for the calculation and the simulation process and its results.

3.1 Development of a SWAT soil database for the upper watershed of River Zala (above Zalaapáti) by incorporating different data sources into GIS

Figure 25: Erosion potential of Zala River catchment



Soil test data and technological data of the crop production process were collected and processed by the county stations of the Plant and Soil Protection Service (Hungary) between the late 70ies and early 90ies for the fields of the large-scale farms. This data- base was maintained by the Central Station of the Plant and Soil Protection Service. Some of the data are outdated but even now useful information may be extracted from the so called AIIR database. The AIIR contains among others soil type, KA (a special test which approximates the plastic limit of soils) and humus content and these data are valuable for the erosion estimates, too.

The AIIR data used in this study were collected by the Zala and Vas County Stations of the Plant and Soil Protection Service between 1984 and 1989. They contain data for the plough layer only since they were used to estimate nutrient demand of arable

crops. The 1:100,000 scale map of the individual fields of the watershed was scanned and aligned to the arable land layer of the CORINE database. The individual fields were digitised as the central point of the field instead of the boundary but the AIIR contains the area of the field, too.

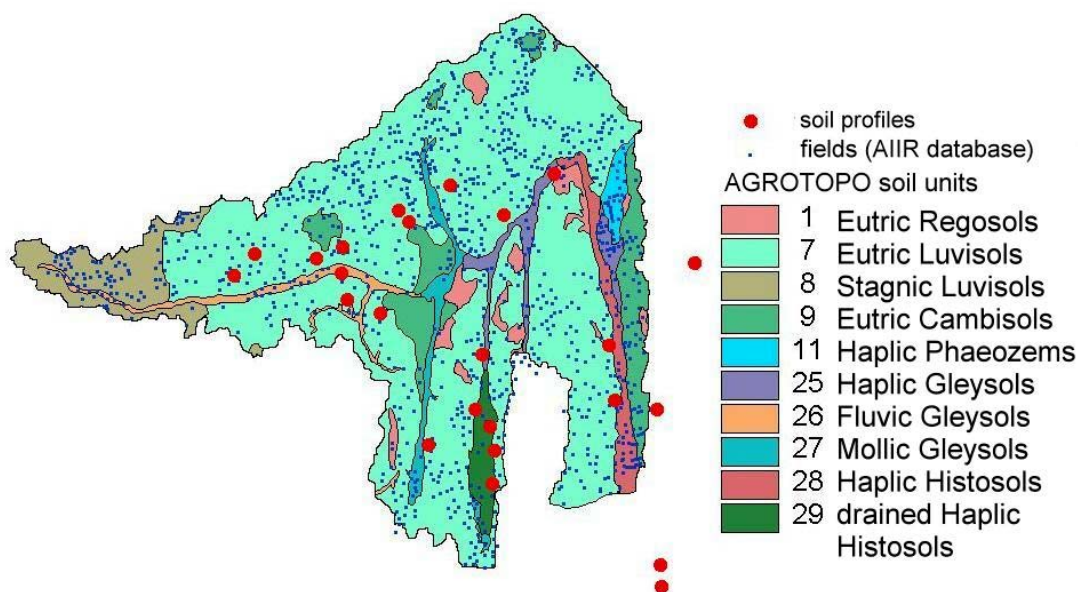
25 soil profiles on 24 sites were described by the Agrolabor-Z Ltd (Zalaegerszeg) between 1993 and 2002. Four of them lies outside of the upper watershed of River Zala but very close to the boundary and these soils have same type as soils within the watershed so they were included in the analysis. The soil profiles were described for different reasons but usually as part of melioration recommendations and they contain beside soil type and major properties of the layers, many physical and chemical data. All of the soil physical data and a few soil chemical data were included in the recent study. Four layers were considered in each profile, so 100 records were included in the analysis with the following variables:

- full particle size analysis
- bulk density
- field capacity
- permanent wilting point
- available water capacity
- gravitational porosity
- adsorption of water vapour
- KA (a special test which approximates the plastic limit of soils)
- saturated hydraulic conductivity
- lime content
- humus content

Pedotransfer functions were calculated from the database and partly from other data, that estimate input data set for the SWAT model mainly with help of KA and the humus content of soils.

The AGROTOPO database of the Research Institute of Soil Science and Agrochemistry of the Hungarian Academy of Sciences was also utilized in the analysis. The original dataset is shown on Figure 26.

Figure 26: Original dataset of the analysis



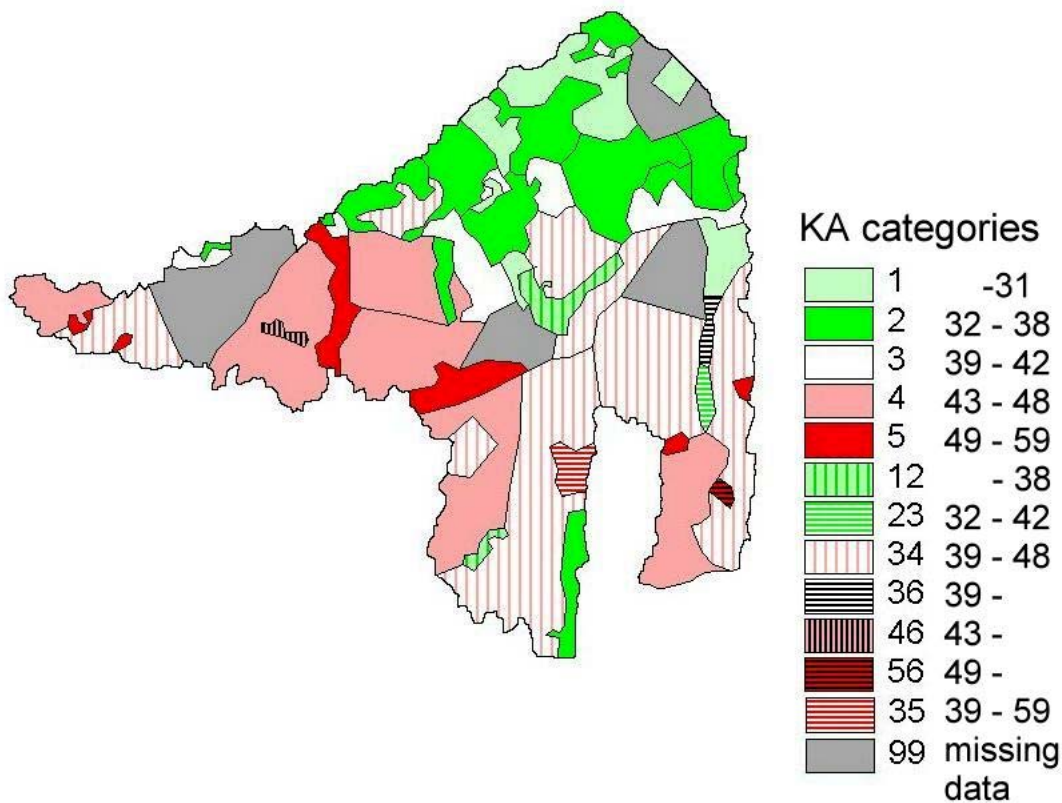
3.1.1 New soil polygons derived from the dataset

The KA data of the AIIR dataset were grouped into the usual categories:

code	physical soil type	KA value
1	sand	-31
2	sandy loam	32-38
3	loam	39-42
4	clayey loam	43-48
5	clay	49-59
6	heavy clay	60-

754 of the 838 AIIR records had average KA data for the arable land fields. 60 soil units were defined based upon the KA categories. Soil units with a single category were defined if possible but in many cases it was not: some of the units contain larger extent of KA values. (e.g. 12, 23, 34, 35, 36, 46, 56). In the double codes both digits are codes of the smallest and largest category characterizing the unit (Figure 27).

Figure 27: Soil units determined upon the KA values

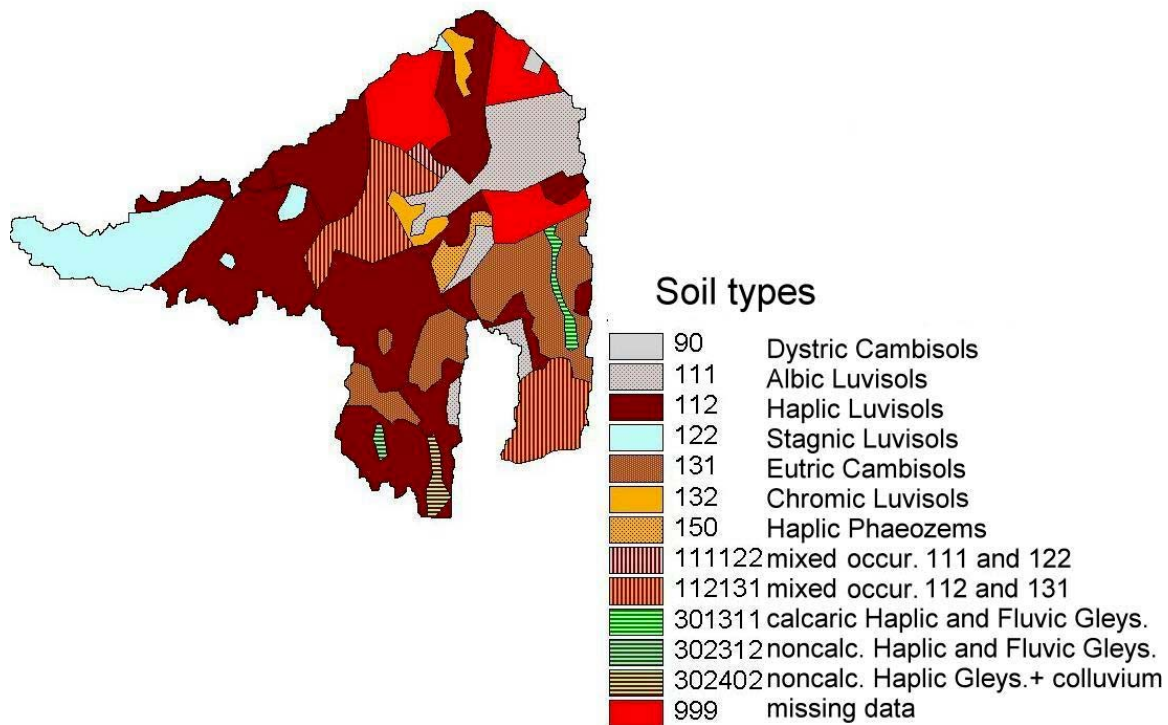


770 of the 838 AIIR records contain data for the major soil type of the field. 39 soil units were defined based upon the soil types. Homogenous units were defined if possible but also here, several units fell into more categories. The soil types considered for the grouping are the following:

code	soil type
90	Dystric Cambisols
111	Albic Luvisols
112	Haplic Luvisols
122	Stagnic Luvisols
131	Eutric Cambisols
132	Chromic Cambisols
150	Haplic Phaeozems
301	calcaric Haplic Gleysols
302	noncalcaric Haplic Gleysols
311	calcaric Fluvic Gleysols
312	noncalcaric Fluvic Gleysols
402	colluvium derived mostly from Luvisols

Other soil types are also present in the database but the number of entries is small so they were not considered in the grouping. Codes for the combined categories contain in their first to third digits and in the fourth to sixth digits the codes of the characteristic soil types (Figure 28).

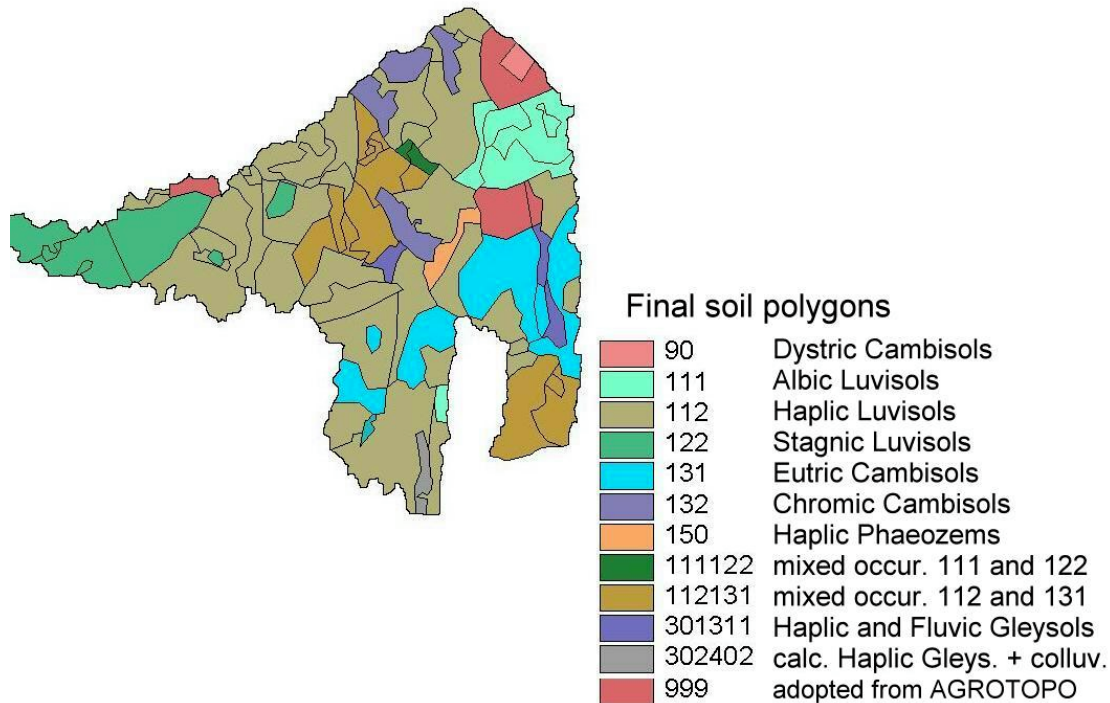
Figure 28: Soil units determined upon the soil types



More than 200 soil polygons were defined by the intersection of the two sets of polygons resulted from the previous groupings. The new soil units were investigated one by one and unified where it was possible and necessary. Finally, 82 polygons were defined on this way. (Figure 28). 3 to 80 records (14 on the average) fell in one unit depending on the size. The areas of the fields falling in one unit were summed up and averages and variances were calculated from the soil test data (KA, humus content, ammonium-lactate soluble K_2O and P_2O_5 content) and calculated data were assigned to the polygons. The compiled data have given the independent variables for the pedotransfer functions (see later) and the result of the calculation has given the input file for the SWAT model. 5 empty units were found in the database in an intermediate phase of the analysis. They had relatively large areas and they missed any AIIR records. These units were investigated based upon the AGROTOPO database, they were split if necessary and partly or entirely unified with the neighbouring similar units, or data of near-falling similar units were assigned to them.

Average data from AGROTOPO were allocated to the units which had still been remaining empty (Figure 29).

Figure 29: Soil polygons as result of the analysis with the indication of soil types



3.1.2 Calculation of pedotransfer functions in sequence of the variables of SWATmodel

SNAM – the name of the soil unit: identifiers of the 82 soil polygons.

NLAYERS – number of layers: 4 in all cases since soil descriptions were done so.

HYDGRP – hydrologic soil groups. They were determined based upon the saturated hydraulic conductivity of all layers as described in SWAT manual. No soil unit has fallen into the category "A" according to the saturated hydraulic conductivity but soils in the first KA category with more than 5 % rock fragment were grouped as "A" hydrologic soil group.

SOL_ZMX - Maximum rooting depth of soil profile (mm). There is no hard pan layer in the upper 150 cm of the profiles described.

ANION_EXCL - Fraction of porosity (void space) from which anions are excluded. As no value for this variable is entered, the model set ANION_EXCL = 0.50.

SOL_CRK - Potential or maximum crack volume of the soil profile expressed as a fraction of the total soil volume. This variable was determined using KA values: it was set 0.00 in KA categories 1, 2, 12 and 3; 0,01 in KA category 34; 0,02 in KA category 4, 35 and 36; and 0,05 in categories 5, 46 and 56.

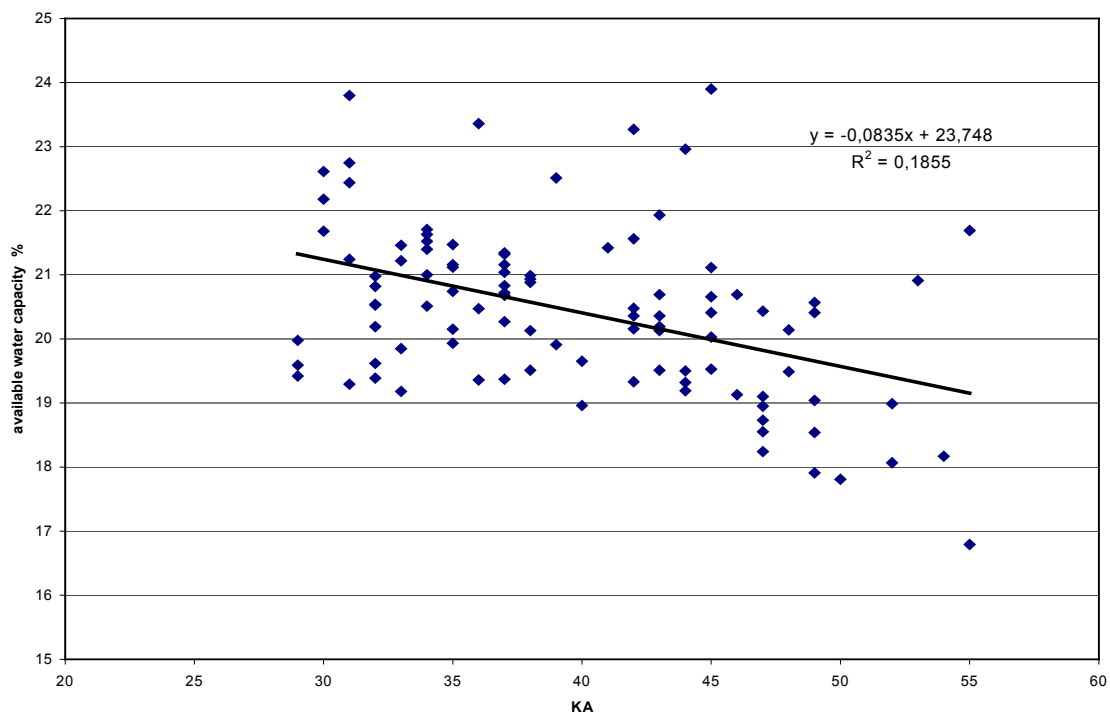
TEXTURE - Texture of soil layer. This data is not processed by the model and the line was left blank.

SOL_Z(layer #) - Depth from soil surface to bottom of layer (mm). There isn't any variable in the soil physical database (description of the profiles) correlating with this variable. Average depth was calculated for soil types which were sufficiently represented in the soil physical database (111,112, 122, 131, 132). The individual values of the profile were generalized and assigned to the soil unit if the soil type from AIIR and of the profile were the same and the average AIIR data (KA, humus) were close to the profile data. (distinguished polygons: No. 5, 14, 15, 27, 32, 49, 61, 751, 76 and 80).

SOL_BD(layer #) - Moist bulk density (Mg/m^3 or g/cm^3). The procedure was the same as at the previous variable (distinguished polygons and polygons with representative soil types). The bulk density of the plough layer is significantly smaller than of the deeper layers, but there is no difference among the deeper layers. The analysis has not shown any significant effect of chemical and other physical properties, or of soil type on this variable.

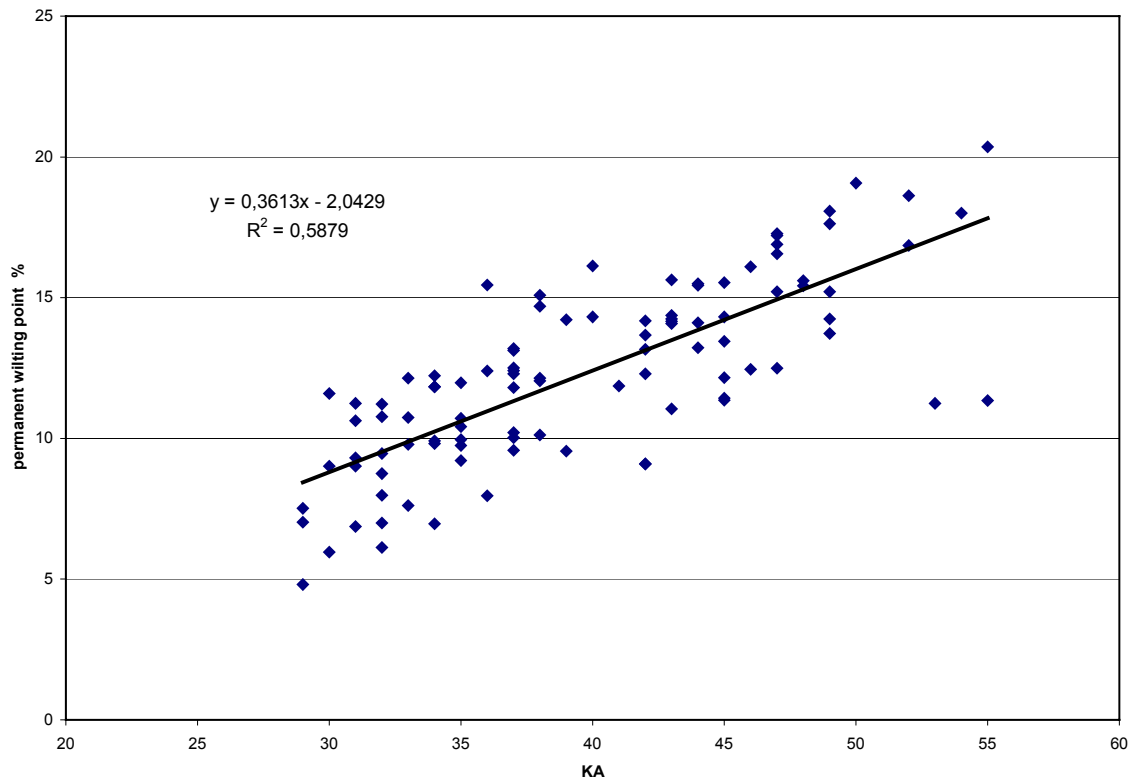
SOL_AWC(layer #) - Available water capacity of the soil layer (mm H_2O /mm soil). The available water capacity, is calculated by subtracting the fraction of water present at permanent wilting point from that present at field capacity ($\text{AWC} = \text{FC} - \text{WP}$). The relationship between AWC and KA in the database is shown on Figure 30.

Figure 30: Available water capacity as function of KA



Our knowledge and published physical data about Hungarian soils (Várallyay, 1989) strongly contradict the relationship on the figure: light sandy soils ($KA \leq 30$) cannot have AWC equal to or higher than 20 % AWC, the procedure of the measurement should have gone wrong in this case. The data do not reflect the general relationship of increasing AWC at increasing KA up to the loamy soils and the decreasing AWC at high KA values (clay and heavy clay) therefore the determiners of AWC (FC and WP) were also investigated (Figure 31 and Figure 32).

Figure 31: Permanent wilting point as function of KA



The values of permanent wilting point at light soils are slightly higher than expected but their relationship with KA is reliable. On the contrary, field capacity data are much higher than expected. Systematic error of measurement can be assumed here. An attempt has been made to reproduce the relationship between AWC and KA as it is evident in the work of Várallyay (1989). Permanent wilting point data were accepted in the calculation and the following rules were applied: humus colloids are very efficient in improving water retention; volume of capillary and micro pores changes with the amount of clay and silt content. The “artificial” variable was calculated on the following way:

$$AWC_{\text{calc}} = \text{TOTPOR} \cdot (1 - \text{SAND}) + 2 \cdot \text{HUMUS}^2 - \text{WP} \quad (14)$$

AWC_{calc} - calculated available water capacity (%)

TOTPOR - total porosity (%)

SAND - sand content (fraction)

HUMUS - humus content (%)

WP - permanent wilting point (%)

Figure 32: Field capacity as function of KA

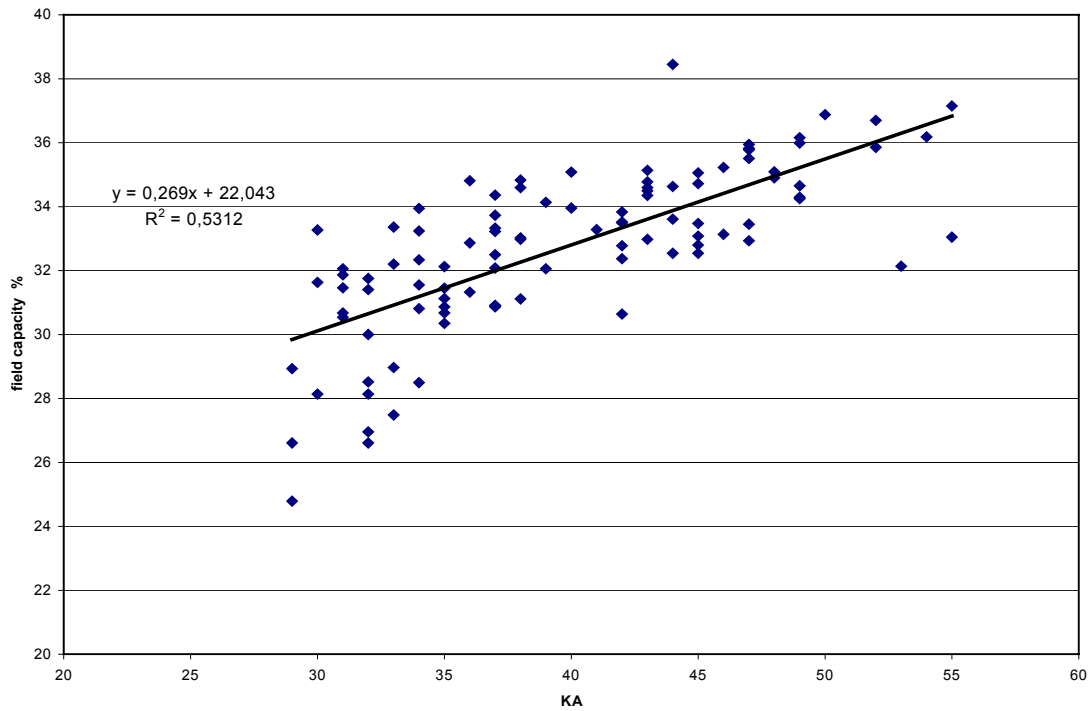
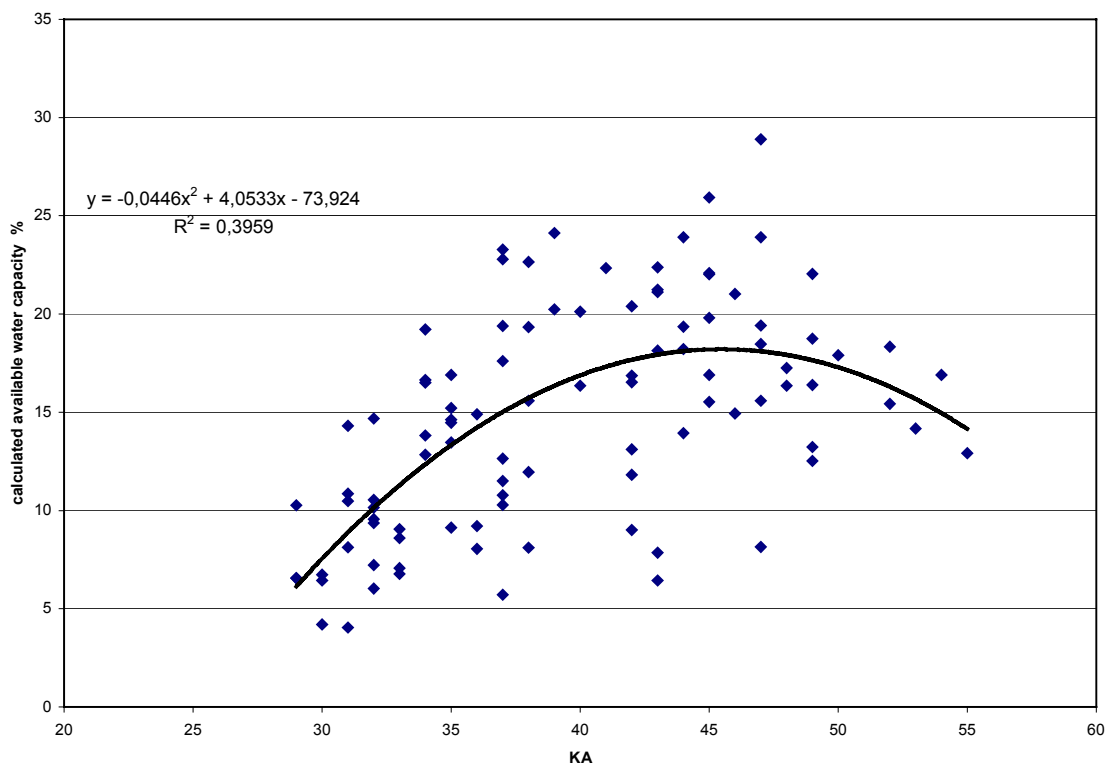


Figure 33: Calculated available water capacity as function of KA



The result of calculation is shown on Figure 32. The variance of data is rather high but the theoretical relationship and table values of Várallyay (1989) are fairly described by the second order polinomial function.

Not surprising that AWC_{calc} has shown good linear relationship with humus since humus was used to calculate it but KA is also a strong determiner although quadratic relationship was not significant. The calculated pedotransfer function is:

$$AWC_{calc} = -9.53 + 6.215 * HUMUS + 0.474 * KA \quad (15)$$

$$R^2 = 0.634$$

Equation (15) was used to calculate the available water capacity in the upper layer (SOL_AWC1) from average KA and humus values for each polygon. Data for the deeper layers (SOL_AWC2-4) were compiled on the following way: ratios of AWC of upper and deeper layers were determined based on the soil physical database for the major soil types as well as for different subgroups and the whole dataset and the appropriate ratios were applied to the polygons. In the distinguished polygons (No. 5, 14, 15, 27, 32, 49, 61, 751, 76 and 80), the actual data of the profile falling on the polygon were generalized and assigned to the polygon.

SOL_K(layer #) - Saturated hydraulic conductivity (mm/hr). This variable is included in the soil physical database and its value depends on KA only:

$$SOL_K = 94.29 * \exp(-0.1218 * KA) \quad (16)$$

$$R^2 = 0.702$$

Equation (16) was used to calculate SOL_K for the upper layer from average KA for each polygon. The procedure described at SOL_AWC was applied in case of deeper layers and distinguished polygons.

SOL_CBN(layer #) - Organic carbon content (% soil weight). Humus content in the plough layer for each polygon is included in the database as average of several fields' data. It was divided by 1.724 to obtain carbon content. The procedure described at SOL_AWC was applied in case of deeper layers and distinguished polygons. The database contains entries from arable land and orchards only. Carbon content in soils of greenland and wood should be higher. Relationships must be sought during the development of the database to better calculate humus content of seminatural areas.

CLAY(layer #) - Clay content (% soil weight). The clay content of the upper layer shows very weak relationship with the other soil properties therefore silt and sand content were expressed as function of the other properties and clay content was calculated as $CLAY = 100 - SILT - SAND$. Clay contents of the deeper layers show very characteristic pattern depending on the soil type so the use of ratios is very appropriate method in order to express clay content of subsoil layers. In case of the distinguished polygons the described method was used (assignment of the data of profiles to the polygons).

SILT(layer #) - Silt content (% soil weight). The percentage of soil particles which have an equivalent diameter between 0.05 and 0.002 mm. The range of silt-sized particles is different from that used in Hungary so the very fine sand fraction (by the Hungarian definition) had to be added to the 0.002-0,02 mm fraction. The following equation had the best fit:

$$SILT = -14.26 + 1.176*KA + 6.171*HUMUS \quad (17)$$

$$R^2 = 0.545$$

Equation (17) was used to calculate the silt content of the upper layer. The procedure described at SOL_AWC was applied in case of deeper layers and distinguished polygons. It is surprising that humus content has a positive significant effect. A possible explanation is that the standard procedure in Hungary do not destroy all the microaggregates and the amount of “surviving” aggregates is proportional to the humus content. This conclusion is the second indication of the weak points of the standard procedure beside field capacity.

SAND(layer #) - Sand content (% soil weight). The percentage of soil particles which have a diameter between 2.0 and 0.05 mm. Linear relationship was calculated between sand content and KA:

$$SAND = -120.26 - 1.943*KA \quad (18)$$

$$R^2 = 0.666$$

Equation (18) was used to calculate the sand content of polygons in the upper layer from KA data. In case of the deeper layer the difference $SAND = 100 - SILT - CLAY$ was used and in case of the distinguished polygons the procedure described at AWC was used.

ROCK(layer #) - Rock fragment content (% total weight). The percent of the sample which has a particle diameter >2 mm, i.e. the percent of the sample which does not pass

through a 2 mm sieve. In case of distinguished polygons the actual rock fragment percentages of the profiles were generalized and assigned to the polygon. In case of polygons (No. 1, 19, 34, 37, 38, 73, 451 and 47), where the AGROTOPO indicated the physical type 7 (not or partly weathered rough material) 5 % rock fragment ratio was assumed in all layers. As the major particle size fractions are calculated as percentages of the soil material without rock fragment., percentages of clay silt and sand had to be recalculated to satisfy the relationship: $CLAY + SILT + SAND + ROCK = 100$.

SOL_ALB(layer #) - Moist soil albedo. The ratio of the amount of solar radiation reflected by a body to the amount incident upon it, expressed as a fraction. Szász (1989) reported that the albedo for sandy soils is between 0.1 and 0.25 and for finer arable soils between 0.15 and 0.3, therefore 0.175 was assigned to the polygons with KA category=1 and 0.225 was assigned to them in all other cases.

USLE_K(layer #) - USLE equation soil erodibility (K) factor (units: 0.013 (metric ton m^2 hr)/(m^3 -metric ton cm)). The USLE K values were calculated from the soil physical database with help of the first equation recommended by the SWAT manual (Wischmeier et al. 1971):

$$K_{USLE} = [(0,00021 * M^{1,14} * (12 - OM) + 3,25 * (c_{soilstr} - 2) + 2,5 * (c_{perm} - 3)] / 100 \quad (19)$$

$$M = (m_{silt} + m_{vfs}) * (100 - m_{clay}) \quad (20)$$

msilt - the percent silt content (0.002-0.05 mm diameter particles),

mvfs - the percent very fine sand content (0.05-0.10 mm diameter particles),

mclay - the percent clay content (< 0.002 mm diameter particles).

OM - percent organic matter content

csoilstr - the soil structure code used in soil classification. It was estimated upon the soil type, KA, and soil layer with help of table in the SWAT manual.

cperm - the profile permeability class. It was determined from the saturated hydraulic conductivities with help of the table in the SWAT manual.

Results from equation (19) was correlated with the variables from the database, only the KA values had significant effect:

$$K_{USLE} = 7.122 \cdot 10^{-2} + 6.277 \cdot 10^{-3} \cdot KA \quad (21)$$

$$R^2 = 0.372$$

The R^2 value is not high but much better than those for the USLE K values calculated differently. The results of the different calculations are not shown. Equation (21) was used to calculate soil erodibility of the upper layers. The procedure described at SOL_AWC was applied in case of deeper layers and distinguished polygons.

SOL_EC(layer #) - Electrical conductivity (dS/m). Not currently active

The compiled dataset was used to run the SWAT model after calibration of runoff.

3.1.3 SWAT model application for Zala River catchment

Based on the developed soil database the Modified Universal Soil Loss Equation (MUSLE) incorporated into the SWAT2000 model was applied for the erosion calculation in the upper Zala River watershed for the period 1997-2001. However, the resolution of the delineated watershed map and the compiled soil map mentioned above were different, therefore an adjustment process was performed. For each sub-basin of the hydrological model an average K-factor (K_{USLE}) was determined and used for the erosion calculations. Beside this, the coarse fragment factor (CFRG) was also set, based on the rock content of the first soil layer. The other soil parameters were only controlled with values calibrated in the hydrological calculations (they fitted right each other), because in MUSLE only the K-values and the rock content appear directly. The soil properties are discussed in detail in the previous sub-chapters. The other catchment properties are presented hereinafter.

Watershed characteristics

The examined upper part of the total watershed is nearly 1500 km². The watershed characteristics which have influence on MUSLE parameters are topography, landuse types, and measures made in the catchment for the reduction of erosion. The topographic conditions are presented in Figure 34. The area has an elevation range between 100 and 300 m over Baltic Sea level. Based on the digital elevation model the average slope and hillslope length values can be calculated for every Hydrological Response Unit (HRU), which are important for the calculation of the topographic factor (LS_{USLE}). The average slope values of the sub-basins are presented in Figure 35. The minimum is 1.3 %, the maximum is 12.8 %, and the average for the total catchment is 6.6 %. For each landuse or cover types a minimum value of the cover factor ($C_{USLE,min}$) can be determined. Based on this value and the simulated growing cycle of each plant type in the HRU during the year, the actual value of the cover factor ($C_{USLE,act}$) can be computed for every day in the simulation period. The landuse map is shown in Figure 36. The majority of the watershed is agricultural area, principally arable land, which is 54 % of the catchment area. Forests are relatively important, since they cover approximately one third of the area. The support practice in the catchment is usually the contour tillage, but in many cases the direction of the ploughing is parallel with the hillslope direction.

Consequently the management practises generally do not protect too much the soils against the erosion. Finally, the main driving forces of erosion are the precipitation and the surface runoff. The measured rainfall and the SWAT simulated surface runoff values are shown in Figure 37 and Figure 38. The yearly average rainfall for each sub-basin was determined based on daily data of different measuring stations in or nearby the watershed. The precipitation varies between 575 and 700 mm/year, the average is 596.4 mm /year. The generated surface runoff values are between 1.5 and 80 mm/year, the mean value is 11.6 mm/year, which is 13 % of the total runoff of the watershed (89.3 mm/year).

Figure 34: Topography of the Zala River catchment

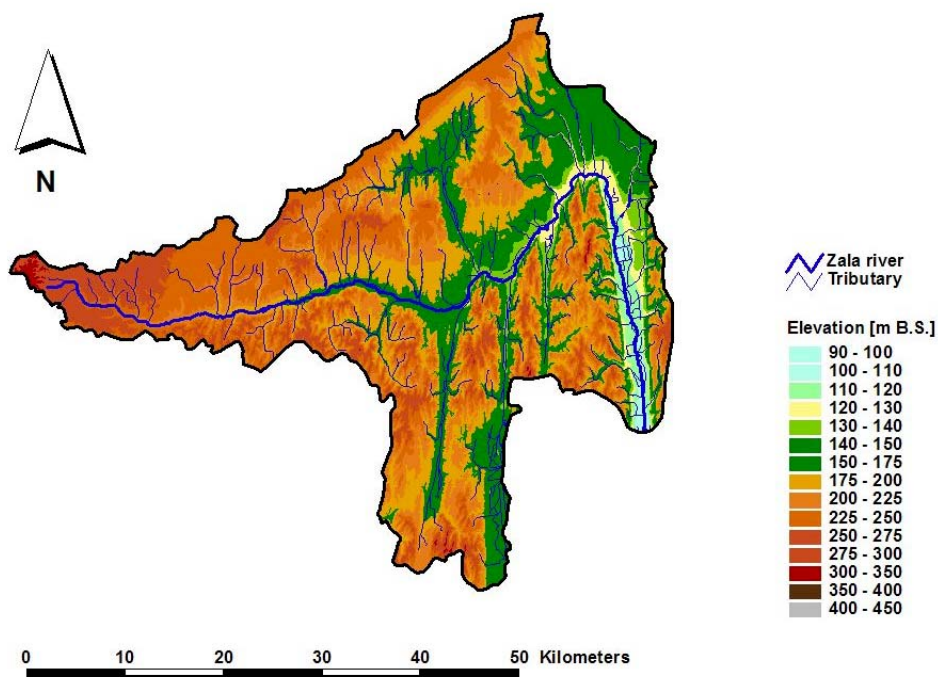


Figure 35: Average slope values of the sub-basins of Zala River

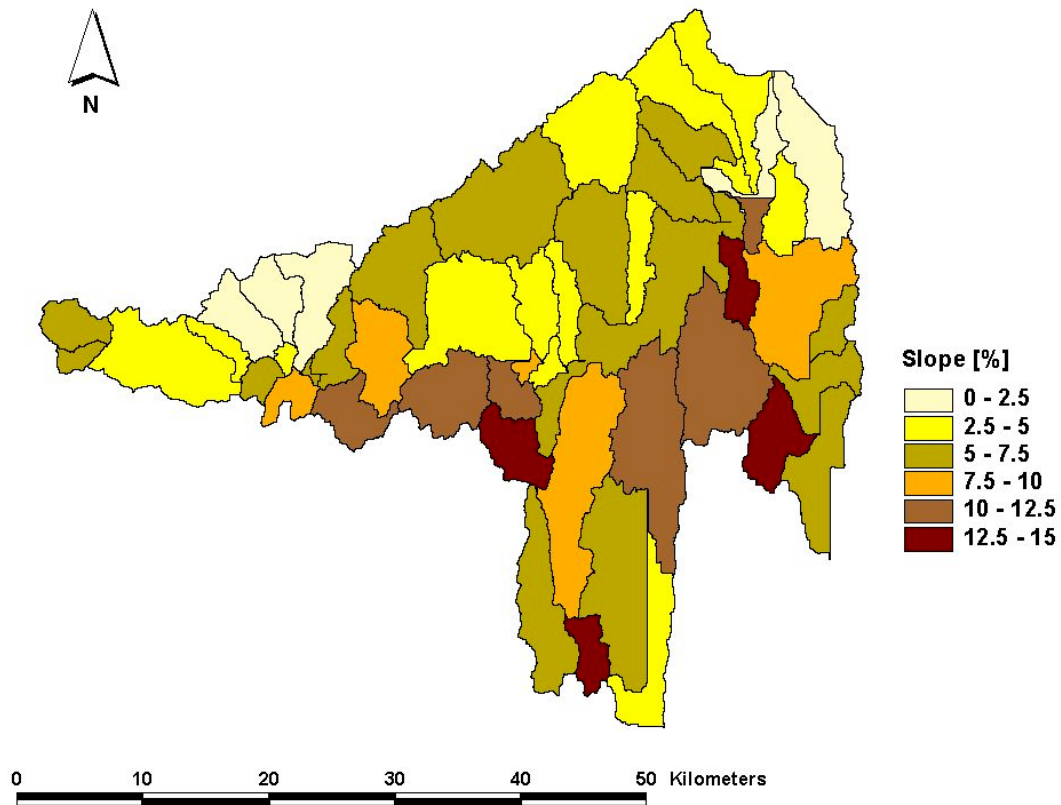


Figure 36: Landuse types in Zala River catchment

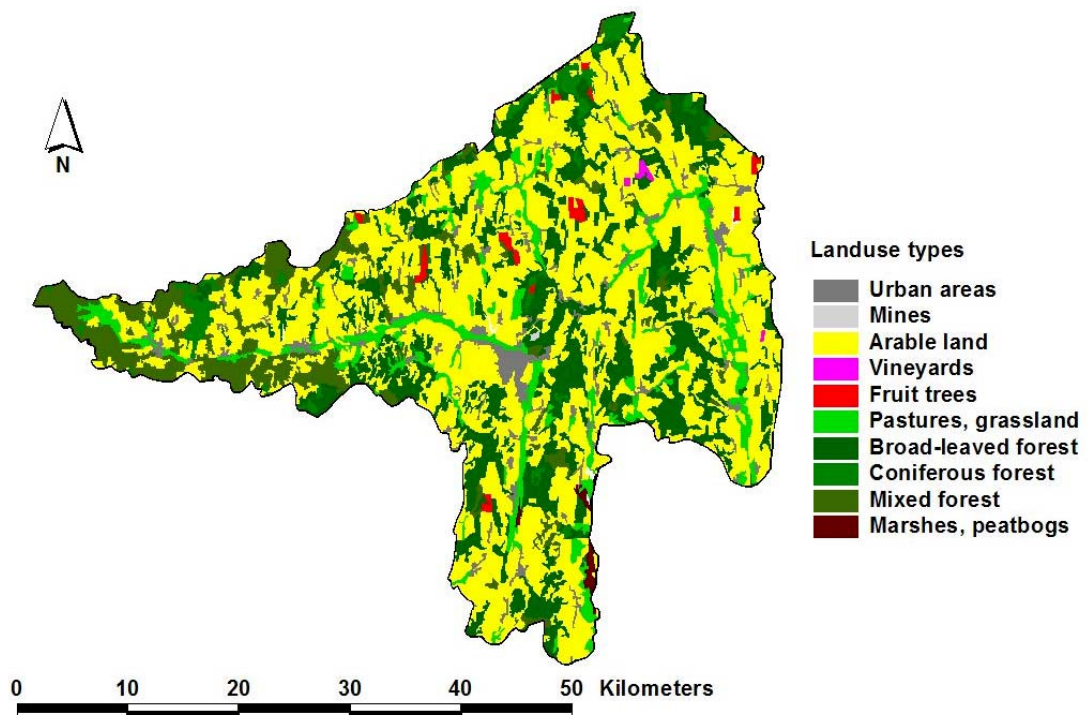


Figure 37: Yearly average precipitation in the sub-basins of the Zala River (1997-2001)

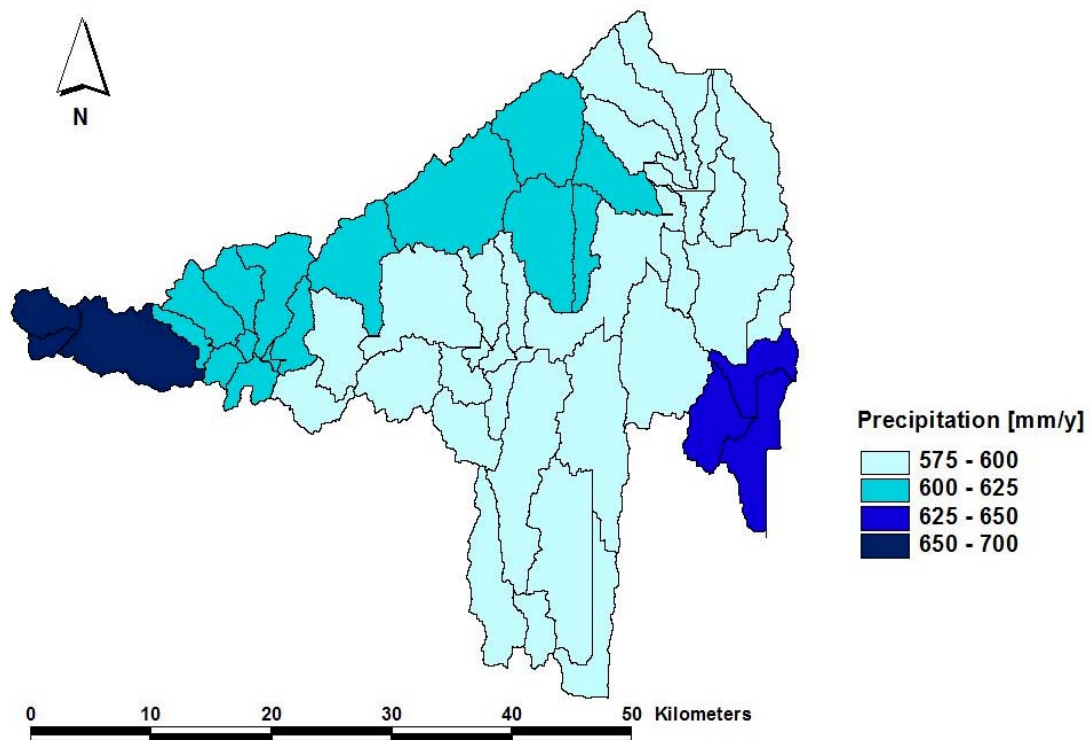
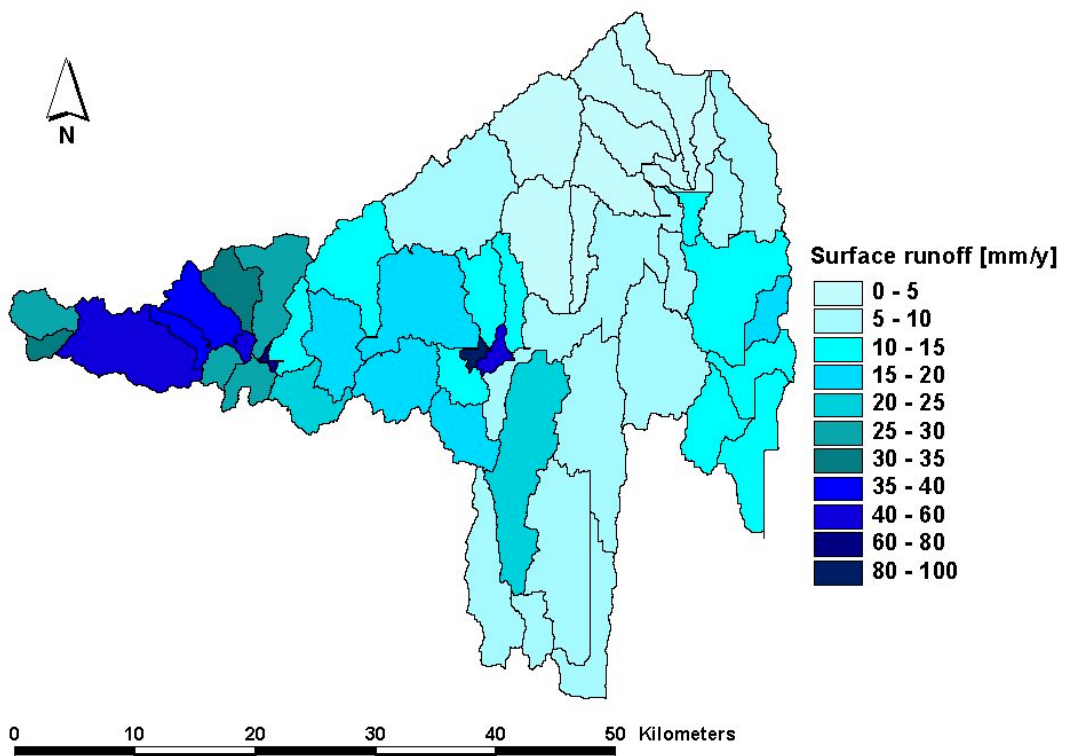


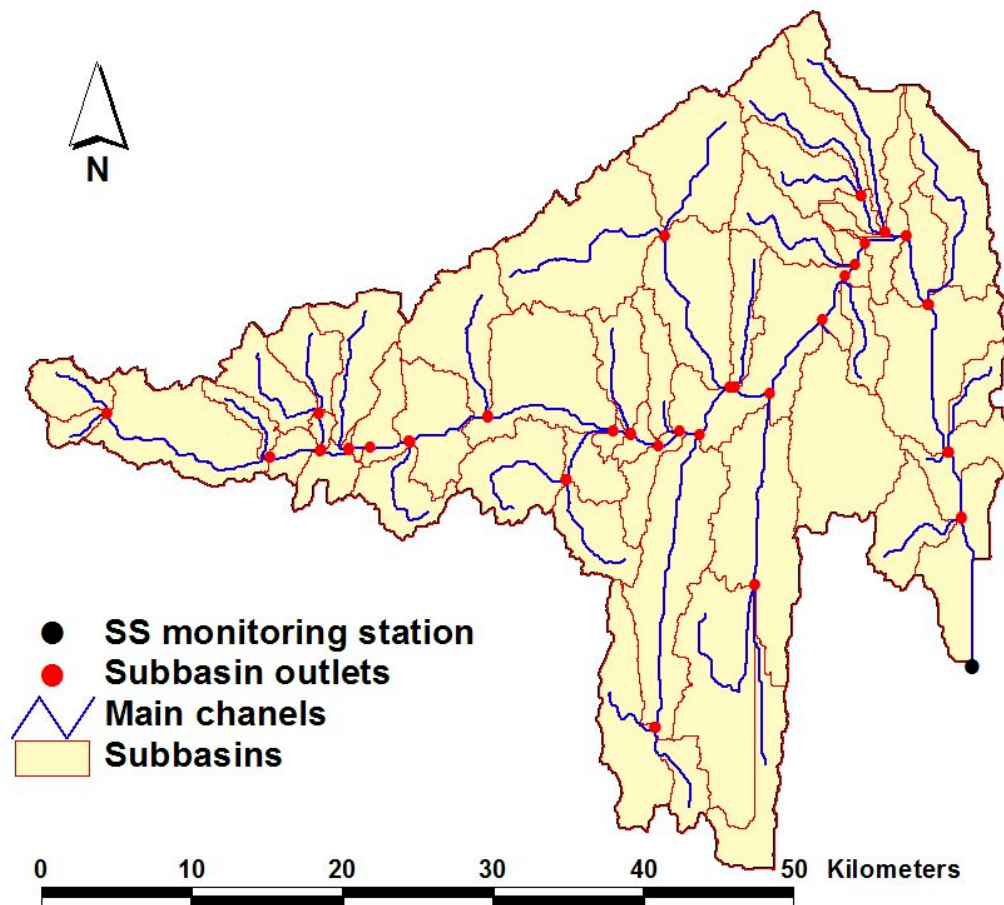
Figure 38: Yearly average surface runoff in the sub-basins of the Zala River (1997-2001)



SWAT application

Based on the calibrated hydrological model the sediment input into the river was simulated using MUSLE for each HRU of every sub-basin. During the simulation the MUSLE-parameters were calibrated in their possible physical range. Unfortunately only one monitoring point with suitable measuring frequency was available in the watershed (at the final outlet), consequently only the sediment load from the total area was controllable, but not the loads from its smaller parts or sub-basins. It is important to note, that the simulated sediment input from the watershed can not be directly compared to the suspended solids (SS) load measured at the outlet, because it contains also the impact of the point sources load, the algae biomass and the sedimentation-resuspension processes. Therefore the suspended solids load arising from the erosion was separated from the measured total SS load. This method is described in the following part. It was assumed about the sedimentation-resuspension processes of the eroded soil material that the net amount is nearly zero in long term, so the total amount of eroded soil entering the river gets out of it. It means that the simulated sediment input caused by erosion already can be compared to the separated sediment load measured at the catchment outlet. The calculated and measured sediment load values were compared at long-term level (5 years average for the period 1997-2001). The watershed delineation with the outlets and the monitoring point are presented in Figure 39.

Figure 39: Watershed delineation for the hydrological and MUSLE calculations of Zala River catchment (including the sub-basin outlets and SS monitoring station)



Data analysis

To determine the suspended solids load at the catchment outlet arising from the erosion a separation method was applied. For the separation of the total measured suspended solids load into load directly from erosion processes and load from other sources (point sources, algae and river bed material) the river flow time series were examined as first step. From the measured time series the main flow components (surface runoff and baseflow) were separated with the DIFGA (Schwarze et al., 2000) separation method. After that the relationship between the measured flow rate and the suspended solids load were examined on days without surface runoff. On these days suspended solids loads can be originated from the point sources loading, the algae biomass and the resuspended sediment and the river discharge is generally low. In the second step of the separation method a correlation was found between the flow rate and the suspended solids load in the period with only baseflow contribution. To decrease the scattering of the values a clustering process was

applied. The corresponding values of flow rate and sediment load were ordered into increasing sequence and every 10 values following each other were integrated into a cluster and averaged. After that a linear correlation was found between the average values. The clustered values and the correlation is shown in Figure 40. Since the loads from point sources are nearly constant and the algae biomass is not significant in this part of the Zala River, the increasing sediment load with the increasing flow rate means the increasing impact of the sediment resuspension.

In the third step this relationship was extended to the days which have surface runoff. It was assumed that this linear correlation is true in this part of flow rates. So on days when there were surface runoff, the suspended solids load arising from point sources and resuspension of the sediment was calculated with the same linear function. This calculated load is called base sediment load. The difference between the total load and the calculated base load is the suspended solids load caused by erosion. In this way the total load can be separated into base- and erosion loads. The result is shown in Figure 41. The 5 years average values based on this separation method are presented in Table 15. The majority (73 %) of the total sediment load originates from erosion with surface runoff and the rest is the amount of suspended solids from point sources and resuspended river bed material.

Figure 40: Correlation between the clustered and averaged discharge and suspended solids load in periods without surface flow

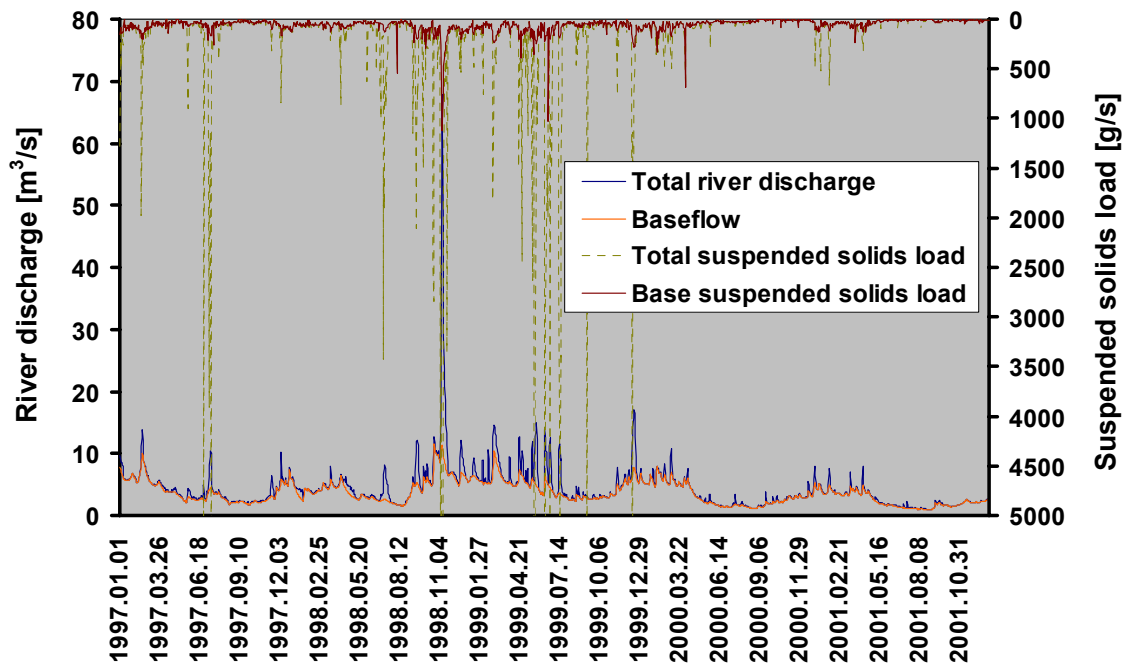


Figure 41: Separated river discharge and sediment load at the final outlet of Zala River catchment

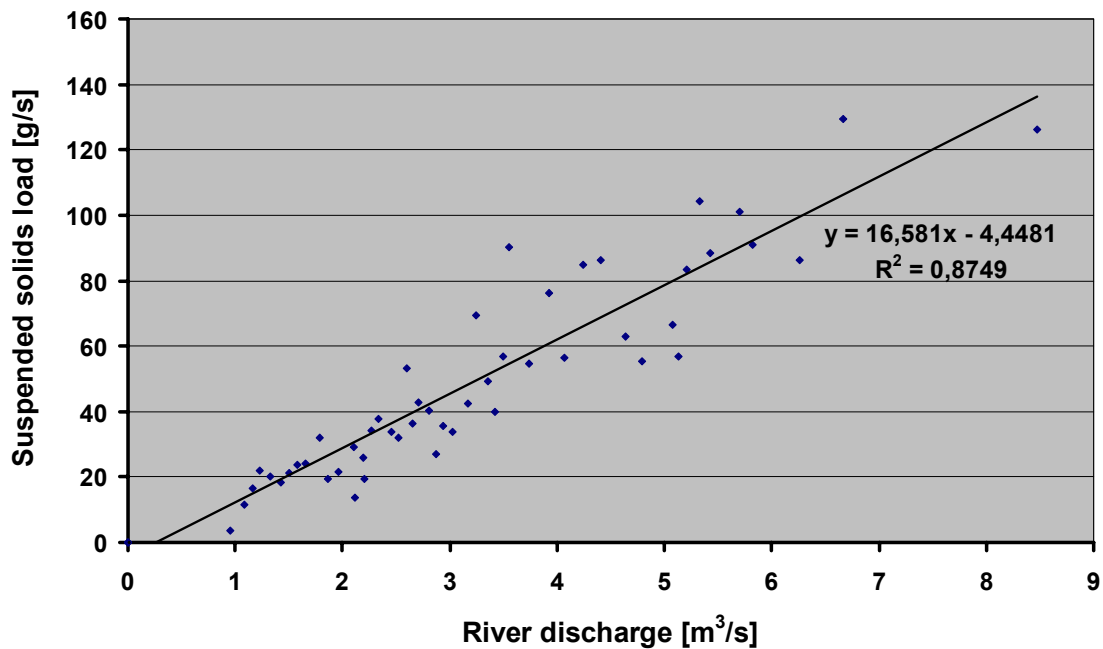


Table 15: Main components of the measured sediment load (1997-2001 average)

Total measured sediment load		6949.8		100.0
Base sediment load	t/y	1887.8	%	27.2
Sediment load caused by erosion		5062.0		72.8

3.1.4 Results, discussion and conclusions

The sediment input from the watershed into the surface water arising from soil erosion was calculated for each HRU of every sub-basin for the period 1997-2001. The results are presented in Figure 42. The sediment input values vary between 10 and 1500 kg/ha/year, the average value is 212 kg/ha/year. This means that the total soil loss from the whole watershed is nearly 32.000 t/year. This value is 50 times less than the average soil loss value mentioned in the introduction. Consequently the retention of the eroded soil in the watershed is very significant, since only 2 % of the total soil loss reaches the river system. However, this value is still much higher than the measured and separated suspended solids load from erosion sources. The comparison of them can be found in Table 16. The calculated sediment input is 6 times higher than the measured erosive sediment load. Accordingly, the model overestimates the sediment input compared to the measured sediment load, if the first assumption is correct, i. e. there is no sediment-retention in the river channel during the high-flow events when erosion usually occurs.

Figure 42: Yearly average sediment input into the surface water in the sub-basins of the Zala River (1997-2001)

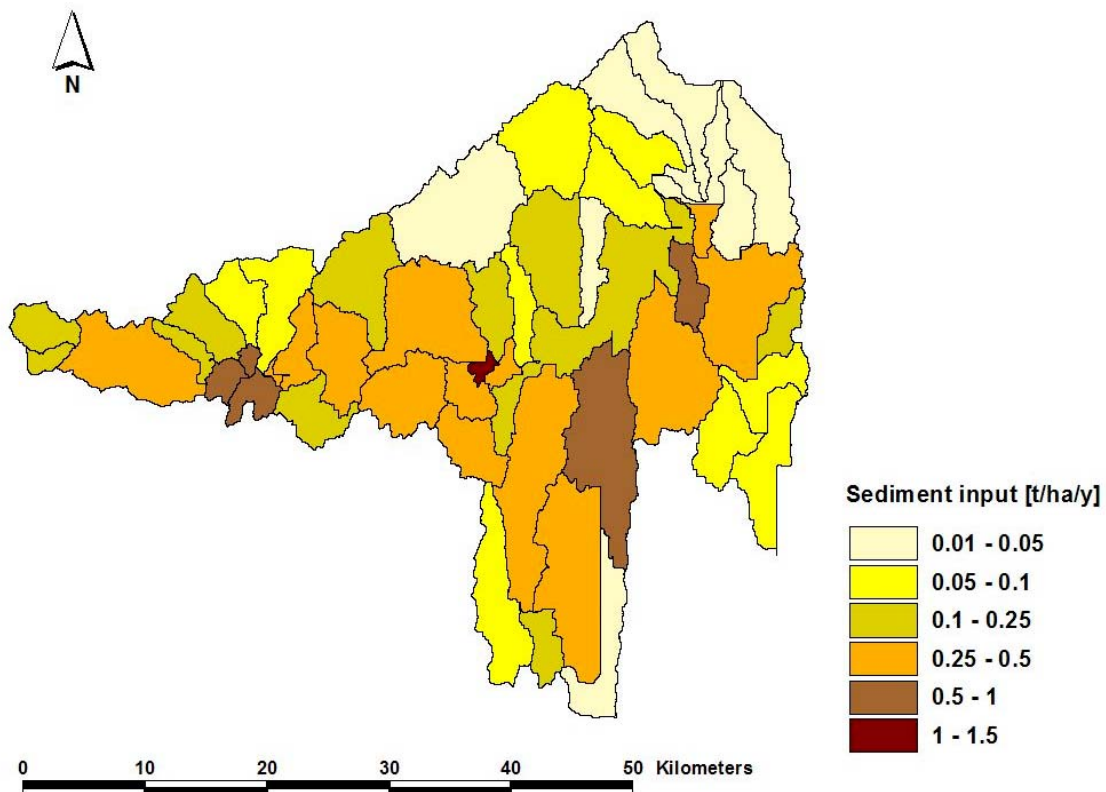


Table 16: Calculated sediment input and measured sediment load (1997-2001 average)

Calculated total sediment input into the surface water		31865.4		0.212
Measured sediment load caused by erosion	t/y	5062.0	t/ha/y	0.034

However, the sediment retention in the river channel is not impossible, if the watershed is not so small, the river net is dense, the examined river section is longer and the river has lower part with lower flow velocity also. The possible sediment retention in the river can be examined with the retention of the particular phosphorus. Since the phosphorus retention takes place by sedimentation, therefore the rate of net sedimentation or retention of the suspended solids is similar to the rate of particular phosphorus retention. Behrendt and Opitz developed an empirical form (Behrendt & Opitz, 1999) to determine the long-term average phosphorus retention in the river systems. This form is analogue to the well known Vollenweider model, which describes the yearly average phosphorus retention of lakes in case of steady state conditions. The phosphorus retention parameter, which gives the relationship

between the total emission of a catchment and the load at the corresponding catchment outlet depends in this approximation on the hydraulic load of the total river system and the specific runoff of the watershed. The first term is the ratio between the yearly average runoff and the area of water surfaces [m/a]. The second value is the ratio of the average river flow rate and the watershed area [l/(km²·s)].

The retention parameter is:

$$R_P = [(a \cdot HL^b) + (a \cdot SR^b)]/2 \quad (22)$$

where:

- R_P the phosphorus retention parameter (t/a),
- HL the hydraulic load of the catchment (m/a),
- SR the specific runoff of the catchment (l/(km²·s)),
- a,b model parameters depending on the catchment size (-).

The parameters are according to the Table 17.

Table 17: Model parameters for the determination of phosphorus retention

	Watershed <1000 km ²		Watershed 1000-10000 km ²		Watershed >10000 km ²	
	HL	SR	HL	SR	HL	SR
a	57.60	41.40	9.30	21.70	26.90	28.9
b	-1.26	-1.930	-0.81	-1.55	-1.25	-1.80

The relationship between the catchment emission and the load at the outlet is:

$$L_P = 1/(1+R_P) \cdot E_P \quad (23)$$

where:

- L_P the yearly average phosphorus load (t/a),

E_P the yearly average phosphorus emission (t/a),

R_P the yearly average phosphorus retention (t/a).

This method has been developed for the calculation of total phosphorus (TP) load from the total TP emission on the watershed. Now, it is assumed, that this relationship is true in the same form for the particular phosphorus also. Consequently this is also suitable to calculate the retention of the sediment in the river channels. Equation (23) can be rearranged:

$$SED = SSL \cdot (1 + R_{SED}) \quad (24)$$

where:

SED the sediment input into the river from the catchment (t/a),

SSL the sediment load at the catchment outlet (t/a),

R_{SED} the retention parameter for the sediment (t/a), which is nearly as same as the phosphorus retention parameter.

With this equation sediment input or emission can be calculated from the measured sediment load.

The results of this approximation are presented in Table 18.

Table 18: Sediment input calculation from the measured sediment load

Yearly average river discharge	m³/s	4.33
Watershed area	km²	1500.91
Water surface area	km²	13.56
Hydraulic load	m/a	10.06
Specific runoff	l/(km²·s)	2.88
Sediment retention parameter	t/a	2.82
Measured sediment load from erosion	t/a	5062.00
Calculated total sediment input by erosion	t/a	19332.58

The simulated sediment load including retention quite fits to the MUSLE value, the latter being 1.5 times higher than the first. So if the channel sediment processes are taken into account, the MUSLE result and the calculated value based on the measurements correlate better. However, it is important to note, that this approximation based on the phosphorus retention has some inaccuracies. First, the retention of the total and particulate phosphorus is different, because the amount of total phosphorus also includes the dissolved phosphorus forms, which is retained to a

smaller extent. Second, also the retention of sediment and phosphorus differ from each other, because the smaller and slowly settling soil particles contain more phosphorus. Beside this, the basic phosphorus sedimentation relationship is a very simple empirical form, which can be extended to other watersheds only with great precaution. Still, this assumption approximates the order of magnitude of sedimentation reasonably. The MUSLE model probably overestimates the sediment input, because the difference between the sediment emission and the measured load is too high. If this amount remained in the river bed, the level of river bottom would increase 2-4 cm annually, which would mean a too fast filling-up process of the channel.

4 SUMMARY

Results of different methodological approaches have been presented in this work. Trying to separate results obtained into different categories may lead to two groups of results:

1. Work to derive basic information on input data for soil erosion modelling for the mesoscale;
2. Work to simulate soil erosion and phosphorus losses within the case study catchments;

4.1 Efforts to derive basic information on input data for soil erosion modelling for the mesoscale

- A procedure has been developed to estimate soil erodibility from soil silt content.
- A procedure has been developed to obtain spatially distributed soil information from a combination of geological maps (spatial information) and soil descriptions (point information). Although this is limited to the special conditions of the Austrian case study areas, the general idea of a combination of geological and pedological information and the practical implementation of this idea may serve for other areas as well.
- A procedure has been developed to link available soil information for Hungary to soil physical input parameters which are necessary for models to simulate different kinds of soil-water relationships.
- It has been shown, that grid dimensions have a strong impact on mean slopes at watershed scale. Based on this analysis a methodology will be presented in Deliverable D 2.2. to account for coarse information on mean watershed slope.
-

4.2 Work to simulate soil erosion and phosphorus losses within the case study catchments;

- Application of the erosion component of SWAT to the case study watersheds resulted in higher simulated sediment yields compared to measured data for the Austrian as well as for the Hungarian case study area. This is mainly due to the fact, that, the model used is not able to simulate sediment yield into the stream

(although claiming to do so) but instead it simulates soil loss on the agricultural fields. Calibration of results is possible in general but made difficult by several factors: i) Cover is a erosion determining component, but in the model it is not possible to get information about mean C-factors (the parameter which determines the effect of cover), II) slope length is important for erosion calculation but is determined in the model in a way (some function of slope) that does not allow the user to interact. Slope lengths may be introduced manually, but in general this information is not available for large watersheds.

- Application of the erosion model MMF to the case study watersheds resulted in sediment yields which are comparable to measured data. However, calibration of the model parameters was necessary beforehand to obtain these results. Calibration also revealed a strong dependency of the MMF model to general climatic conditions, i.e. parameterisation of the runoff component was different for the different case study areas investigated. However, the general possibilities of interfering in the code and the parameter values was easier, as the system was only dealing with erosion and the temporal resolution was monthly.
- Both models were able to identify critical subwatersheds within the Ybbs catchment.
- A comparison of measured P losses with P losses simulated with SWAT revealed a tendency of SWAT, to diminish P concentrations in the soil very rapidly. The concentrations of P exported with the sediment were lower compared to measured data. Simulated P loads overestimated actual P loads for those subwatersheds, where sediment yield had been overestimated.
- The MMF model was also coupled with a routine to calculate P load for the Austrian case study areas. For subbasins with a good approximation in sediment yield in most of the cases also a good simulation of P loads could be reached.
- Although the investigated case study areas already are large and data gathering was one major task of modelling, they are still small compared to the Danube river basin. The question arises, as to which extent modelling approaches like the ones that have been used may be applied to such enormous areas. In that context two problems arise: a) data availability at transnational scale is very restricted and heterogeneous even at the level of case study areas (see available soil information for Austria and Hungary). b) application of dynamic routing of soil loss within watersheds such as demonstrated with the MMF model is restricted to

areas with sufficient resolution of DEM's (as main driving force of runoff) and limited size (because of computation time). These two constraints limit the applicability of the used models outside the so called case study areas.

- However, the MMF model may now be applied within the case study areas to answer questions on the effects of landuse changes or changes in cultivation practices or even climatic changes on soil erosion and surface runoff.

5 REFERENCES

- AGROBER Ltd. (1995): Study of water quality protection, melioration and afforestation in Lake Balaton Watershed. Manuscript. Ministry of Agriculture, Budapest, Hungary.
- Arnold, J. et al. (2000): Soil and Water Assessment Tools. Theoretical documentation. Agricultural Research Service, Temple, Texas, The U.S.A.
- Auerswald K. (1997): In: Botschek J. (1999): Zum Bodenerosionspotetial von Oberflächen und Zwischenabfluss. Bonner Bodenkundl. Abhandlungen, 29, p.61.
- Behrendt, H. et al. (2000): Modeling of Nutrient Emissions into the River Systems. Theoretical documentation. Institute of freshwater Ecology and Inland Fisheries, Berlin, Germany.
- BFL (1999): Bundesamt und Forschungszentrum für Landwirtschaft – Erläuterungen zur Bodenkarte 1:25000 – Eisenstadt. Bundesministerium für Land- und Forstwirtschaft.
- Bundesamt und Forschungszentrum für Landwirtschaft (1996): Burgenländische Bodenzustandsinventur.
- Bundesanstalt für Bodenwirtschaft (1994): Niederösterreichische Bodenzustandsinventur, Amt der Niederösterreichischen Landesregierung (eds.), Wien.
- DeRose R.C., I.P.Prosser, L.J.Wilkinson, A.O.Hughes, W.J.Young (2002): Regional patterns of erosion and sediment and nutrient transport in the Mary river catchment, Queensland. Technical Report 37/02, CSIRO Land and Water.
- ESB - European Soil Bureau, (1998). Georeferenced Soil Database for Europe. EUR 18092 EN.
- Fachbeirat für Bodenfruchtbarkeit und Bodenschutz (1999): Richtlinien für die sachgerechte Düngung. Bundesministerium für Land- und Forstwirtschaft.
- Jones C.A., C.V. Cole, A.N. Sharpley, J.R. Williams (1984): A simplified soil and plant phosphorus model: I. Documentation. Soil Sci.Soc.Am.J., 48, 800-805.
- Kirkby, M.J. (1976): Hydrogical slope models: The influence of climate. In: Derbyshire, E. (Ed.), Geomorphology and Chlimate. Wiley, London, pp. 247-267.
- LVA (1971): Landwirtschaftlich-chemische Bundesversuchsanstalt, Bodenkartierung und Bodenwirtschaft – Erläuterungen zur Bodenkarte 1:25000 – Mattersburg. Bundesministerium für Land- und Forstwirtschaft.

- Meyer M. (1997): Erprobung und Anwendung von Methoden zur einzugsgebietsbezogenen Modellierung der Phosphatdynamik terrestrischer Ökosysteme. <http://www.ecology.uni-kiel.de/~ernst/martin>
- Morgan (2001): A simple approach to soil loss prediction: a revised Morgan-Morgan-Finney model. *Catena*, 44, 305-322.
- Morgan, Morgan, Finney (1984): A predictive model for the assessment of soil erosion risk. *Jour.Agric.Eng.Research*, 30, 245-253.
- Neitsch S.L., J.G. Arnold, J.R. Kiniry, J.R. Williams (2001): Soil and Water Assessment Tool Theoretical Documentation. Grassland, Soil and Water Research Laboratory, ARS, Temple, Texas.
- ÖNORM L 1087 (1993): Bestimmung von pflanzenverfügbarem Phosphat und Kalium nach der Calcium-Acetat-Lactat (CAL)-Methode. Österreichisches Normungsinstitut.
- Risse L.M., M.A. Nearing, A.D. Nicks and J.M. Laflen (1993). Error Assessment in the Universal Soil Loss Equation. *Soil Sci.Soc.Am.J.*, 57, 825-833.
- Salamin, P. (1982): Environmental protection related to the erosion. Manuscript. Budapest University of Technology, Budapest, Hungary.
- Schmidt, J., Werner, M.v., Michael, A. (1996): EROSION 2D/3D, Modellgrundlagen und Bedienungsanleitung, Band 1-3, Freiburg
- Schneider W., P.Nelhiebl, G.Aust, M.Wandl, O.H. Danneberg (2001): die landwirtschaftliche Bodenkartierung in Österreich. *Mitt.d.Österr.Bodenkundl.Ges.*, 62, 39-67.
- Schwarz S., M. Englisch, K. Aichberger, A. Baumgarten, W.Blum, O. Danneberg, G. Glatzel, S. Huber, W. Kilian, E. Klaghofer, O. Nestroy, A. Pehamberger, J. Wagner and M. Gerzabek (2001a). Bodeninformationen in Österreich – aktueller Stand und Ausblick. *Mitt. der Österr. Bodenkundl.Ges.*, 62, 185-216.
- Schwarz S., S. Freudenschuss, S. Huber, A. Riss, I. Schreier; M. Tulipan, M. Weber (2001b): Das österreichweite Bodeninformationssystem BORIS - Aufbau und Auswertungen. *Mitt. d. dt. Bodenkundl. Ges.*, 96, 777-778.
- Schwarze, R. et al. (2000): Difference Time Series Analysis Method. Theoretical documentation. Institution of Hydrology and Meteorology, University of Technology, Dresden, Germany.
- Schwertmann, U., W. Vogl u. M.Kainz, 1987: Bodenerosion durch Wasser. Ulmer Verlag.

- Sharpley A.N., S.A. Jones, C. Gray, C.V. Cole (1984): A simplified soil and plant phosphorus model: II. prediction of labile, organic and sorbed phosphorus. *Soil Sci.Soc.Am.J.* 48, 805-809.
- Spiegel H., Th. Lindenthal, M. Mazorek, A. Ploner, A. Köchl, B.Freyer (2001): Ergebnisse von drei 40-jährigen P-Dauerversuchen in Österreich. 1. Mitteilung: Auswirkungen ausgewählter P-Düngerformen und -mengen auf den Ertrag und die $P_{CAL/DL}$ -Gehalte im Boden. *Die Bodenkultur*, 52,1, 3-17.
- Torri D., J.Poesen, F.Monaci, E.Busoni (1994): Rock fragment content and fine soil bulk density. *Catena*, 23, 65-71.
- Van Deursen, W.P.A. (1995). *Geographical Information Systems and Dynamic Models: development and application of a prototype spatial modelling language*. Doctor's dissertation, Utrecht University
(<http://www.geog.uu.nl/pcraster/pcraster.html>)
- Williams, J.R. (1982): Testing the modified Universal Soil Loss Equation. In: Proceedings of the Workshop on estimating erosion and sediment yield on rangelands. Tuscon, Arizona, March 7-9, 157-165.
- Wischmeier W.H., J.V. Mannering (1969): Reallion of soil properties to its erodibility. *Soil Sci.Soc.Am.Proc.*, 33, 131-137.
- Wischmeier, W.H. and D.D. Smith (1978): Predicting rainfall erosion losses - a guide to conservation planning. U.S. Department of Agriculture, Agriculture Handbook No. 537.
- Wolkerstorfer G. (2002): Vergleich zweier Bodenerosionsmodelle –Morgan Morgan Finney MMF und SWAT anhand des Einzugsgebietes der Ybbs. Diplomarbeit Universität Wien.
- Yoder D.C., G.R. Foster, G.A.Weesies, K.G. Renard, D.K.McCool and J.B. Lown (2001). Evaluation of RUSLE soil erosion model. Southern Cooperative Series Bulletin. 26 Feb. 2003 <<http://www3.bae.ncsu.edu/Regional-Bulletins/Modeling-Bulletin/rusle-yoder-001016.html>>

6 APPENDIX

Values which had been used for the different input parameters of the MMF model are given here.

Table 19: Bulk densities (Mg m^{-3}) for the different land use units (for coding see Table 4) and months

Month	Code												
	15	1	2	3	4	6	7	8	9	10	11	12	13
Jan.	1.36	2.5	2.5	1.8	2.5	2.5	2.5	2.5			1.36	1.36	2.5
Feb.	1.36	2.5	2.5	1.8	2.5	2.5	2.5	2.5			1.36	1.36	2.5
Mar.	1.32	2.5	2.5	1.8	2.5	2.5	2.5	2.5			1.32	1.32	2.5
Apr.	1.3	2.5	2.5	1.8	2.5	2.5	2.5	2.5			1.3	1.3	2.5
May	1.3	2.5	2.5	1.8	2.5	2.5	2.5	2.5			1.3	1.3	2.5
Jun.	1.25	2.5	2.5	1.8	2.5	2.5	2.5	2.5			1.25	1.25	2.5
Jul.	1.25	2.5	2.5	1.8	2.5	2.5	2.5	2.5			1.25	1.25	2.5
Aug.	1.25	2.5	2.5	1.8	2.5	2.5	2.5	2.5			1.25	1.25	2.5
Sep.	1.4	2.5	2.5	1.8	2.5	2.5	2.5	2.5			1.4	1.4	2.5
Oct.	1.4	2.5	2.5	1.8	2.5	2.5	2.5	2.5			1.4	1.4	2.5
Nov.	1.36	2.5	2.5	1.8	2.5	2.5	2.5	2.5			1.36	1.36	2.5
Dec.	1.36	2.5	2.5	1.8	2.5	2.5	2.5	2.5			1.36	1.36	2.5

To take the different soil characteristics into account we split bulk densities for agriculturally used areas according to the different soil types (Table 20). Similarly soil cohesion values were given (Table 21).

Table 21: Soil cohesion values (kPa) for the different soil units and months; Ht = Hochterasse (High terrace), Nt = Niederterasse (Low terrace); Mol = Molasse (tertiary sediment), Mor = Moräne (Moraine); Fp = Au (Floodplain); Flysch = Flysch, Fen = Moor (Fen), Lime = Kalk (Lime); the terms 15°, 15°-25° and 25° refer to the slope of the area.

Amstetten				St Peter					Gaming									
Month	Ht	Mol	Nt	Fp	Ht	Mol	Nt	Fp	Flysch	Ht	Fp	Flysch < 15°	Flysch > 15°	Mor	Fen	Lime < 15°	Lime 15-25°	Lime > 25°
1	17	17	17	17	17	17	17	17	17	17	8	8	17	17	44	17	17	44
2	9	9	9	9	9	9	9	9	9	9	7	7	9	9	33	9	9	33
3	5	5	5	5	5	5	5	5	5	5	4	4	5	5	14	5	5	26
4	3	3	3	3	3	3	3	3	3	3	3	3	3	3	10	3	3	9
5	3	3	3	3	3	3	3	3	3	3	3	3	3	3	10	3	3	9
6	6	6	6	6	6	6	6	6	6	6	7	7	6	6	29	6	6	29
7	9	9	9	9	9	9	9	9	9	9	7	7	9	9	33	9	9	33
8	9	9	9	9	9	9	9	9	9	9	7	7	9	9	33	9	9	33
9	3	3	3	3	3	3	3	3	3	3	3	3	3	3	10	3	3	9
10	3	3	3	3	3	3	3	3	3	3	3	3	3	3	10	3	3	9
11	6	6	6	6	6	6	6	6	6	6	7	7	6	6	29	6	6	29
12	9	9	9	9	9	9	9	9	9	9	7	7	9	9	33	9	9	33

Table 22: Canopy cover values (0-1) for the different land use units and months

Month	Code												
	15	1	2	3	4	6	7	8	9	10	11	12	13
Jan.	1	1	1	0	1	1	1	1	0	0	1	0.5	1
Feb.	1	1	1	0	1	1	1	1	0	0	1	0.5	1
Mar.	1	1	1	0	1	1	1	1	0.02	0	1	0.5	1
Apr.	1	1	1	0	1	1	1	1	0.05	0	1	0.5	1
May	1	1	1	0	1	1	1	1	0.33	0.02	1	0.5	1
Jun.	1	1	1	0	1	1	1	1	0.8	0.12	1	0.5	1
Jul.	1	1	1	0	1	1	1	1	1	0.6	1	0.5	1
Aug.	1	1	1	0	1	1	1	1	0.9	0.82	1	0.5	1
Sep.	1	1	1	0	1	1	1	1	0	0.85	1	0.5	1
Oct.	1	1	1	0	1	1	1	1	0	0.82	1	0.5	1
Nov.	1	1	1	0	1	1	1	1	0	0	1	0.5	1
Dec.	1	1	1	0	1	1	1	1	0	0	1	0.5	1

Table 23: Ground cover values (0-1) for the different land use units and months

Month	Code												
	15	1	2	3	4	6	7	8	9	10	11	12	13
Jan.	1	1	1	0	1	1	0.7	0.8	0	0	1	0.5	1
Feb.	1	1	1	0	1	1	0.7	0.8	0	0	1	0.5	1
Mar.	1	1	1	0	1	1	0.9	0.9	0	0	1	0.5	1
Apr.	1	1	1	0	1	1	0.9	0.9	0.02	0	1	0.5	1
May	1	1	1	0	1	1	0.9	0.9	0.05	0	1	0.5	1
Jun.	1	1	1	0	1	1	0.9	0.9	0.05	0	1	0.5	1
Jul.	1	1	1	0	1	1	0.9	0.9	0.1	0.1	1	0.5	1
Aug.	1	1	1	0	1	1	0.9	0.9	0.1	0.4	1	0.5	1
Sep.	1	1	1	0	1	1	0.9	0.9	0.1	0.4	1	0.5	1
Oct.	1	1	1	0	1	1	0.9	0.9	0	0.4	1	0.5	1
Nov.	1	1	1	0	1	1	0.7	0.8	0	0	1	0.5	1
Dec.	1	1	1	0	1	1	0.7	0.8	0	0	1	0.5	1